Bioactive Materials 6 (2021) 4301–4318

Contents lists available at ScienceDirect

Bioactive Materials

journal homepage: www.sciencedirect.com/journal/bioactive-materials

Photoactivatable nanogenerators of reactive species for cancer therapy

Xiaohua Zheng, Ph.D. [a], Yilan Jin [a,b], Xiao Liu [a], Tianqing Liu, Ph.D. [c], Weiqi Wang, Ph.D. [a,b,*], Haijun Yu, Ph.D. [b,**]

[a] School of Pharmacy, Nantong University, Nantong, Jiangsu Province, 226001, China
[b] State Key Laboratory of Drug Research & Center of Pharmaceutics, Shanghai Institute of Materia Medica, Chinese Academy of Sciences, Shanghai, 201203, China
[c] NICM Health Research Institute, Western Sydney University, Westmead, Australia

ARTICLE INFO

Keywords:
Reactive oxygen species
Reactive nitrogen species
Alkyl radicals
Carbon monoxide
Phototherapy

ABSTRACT

In recent years, reactive species-based cancer therapies have attracted tremendous attention due to their simplicity, controllability, and effectiveness. Herein, we overviewed the state-of-art advance for photo-controlled generation of highly reactive radical species with nanomaterials for cancer therapy. First, we summarized the most widely explored reactive species, such as singlet oxygen, superoxide radical anion ($O_2^{\bullet-}$), nitric oxide ($^{\bullet}NO$), carbon monoxide, alkyl radicals, and their corresponding secondary reactive species generated by interaction with other biological molecules. Then, we discussed the generating mechanisms of these highly reactive species stimulated by light irradiation, followed by their anticancer effect, and the synergetic principles with other therapeutic modalities. This review might unveil the advantages of reactive species-based therapeutic methodology and encourage the pre-clinical exploration of reactive species-mediated cancer treatments.

1. Introduction

Reactive species are necessary regulatory substances in various physiological functions [1,2]. As the most abundant components in organisms, the common nonmetal reactive species are generally based on oxygen, nitrogen, carbon, sulfur, etc [3–5]. Reactive species include a collective term of non-radical molecular forms (hydrogen peroxide (H_2O_2), CO, etc.) and the radical forms. Radicals refer to those atoms, ions, or molecules that contain unpaired electrons in the outermost electron orbitals, such as alkyl radical [6], nitric oxide ($^{\bullet}NO$) [7,8], peroxynitrite anion ($ONOO^-$) [9], hydroxyl radical ($^{\bullet}OH$) [10], chlorine radical ($^{\bullet}Cl$) [11] and superoxide radical anion ($O_2^{\bullet-}$) [12]. These reactive species generally possess a short lifetime due to their high reactivity [13,14]. Low concentrations of reactive species exhibit beneficial effects in immune response and maintenance of redox homeostasis and normal metabolisms of the cells [15–17]. In contrast, abnormal levels of reactive species can also lead to oxidative stress and even cell death by irreversibly damaging biofunctional macromolecules (nucleic acid, lipids, and proteins) [18,19]. The human body has an antioxidant defense system, comprising some small-molecule antioxidants (*e.g.* Vitamin C and glutathione) and antioxidant enzymes (superoxide dismutases, catalase, glutathione peroxidases, peroxiredoxins, etc.) [20–22]. These antioxidants can abolish reactive species-induced oxidative stress to maintain the redox balance of the biological system [23].

Accumulated evidence has indicated that cancer cells possessed a high level of reactive species [24]. To keep the redox balance, most cancer cells have to generate more endogenous antioxidants [25]. The flexible alteration ability of redox status reduced the therapeutic effect of chemotherapy and radiotherapy on malignant tumor cells. Interestingly, some experimental results suggested that reactive species could exhibit higher damaging effects to cancer cells than normal cells [26]. The preferential inhibition outcome might be attributed to the direct suppression of reactive species to endogenous antioxidants in cancer cells. Despite reactive species-based nanomedicine have intrinsic advantages, reactive species-based cancer therapy is restricted by several limitations: (1) oxygen dependence limited the therapeutic effects to hypoxic tumors; (2) the short absorption wavelength of photoactivatable nanogenerators kept traditional reactive species-based nanoplatform from eliminating deep-seated tumors; (3) undesirable side effects derived from the nonspecific distribution of nanogenerators remain an issue. Regarding these concerns, researchers have been devoted to designing and creating theranostic platforms derived from

Peer review under responsibility of KeAi Communications Co., Ltd.
* Corresponding author. School of Pharmacy, Nantong University, Nantong, Jiangsu Province, 226001, China.
** Corresponding author.
E-mail addresses: wwq1990@ntu.edu.cn (W. Wang), hjyu@simm.ac.cn (H. Yu).

https://doi.org/10.1016/j.bioactmat.2021.04.030
Received 27 December 2020; Received in revised form 30 March 2021; Accepted 17 April 2021

Abbreviations

NPs	Nanoparticles
PTT	Photothermal therapy
NMOFs	Nanoscale metal-organic frameworks
ACQ	Aggregation caused quenching
AIE	Aggregation-induced emission
FRET	Förster resonance energy transfer
NIR	Near-infrared
CONs	Covalent organic nanosheets
EPR	Enhanced permeability and retention
DOX	Doxorubicin
UCNPs	Upconversion nanoparticles
TPZ	Tirapazamine
OVA	Ovalbumin
AuNCs	Au nanocages
PDT	Photodynamic therapy
PSs	Photosensitizers
POP	Porous organic polymer
SPNs	Semiconducting polymer nanoparticles
CA-IX	carbonic anhydrase IX
P-gp	P-glycoprotein
PTX	Paclitaxel
iNOS	•NO synthase
DTX	Docetaxel
BSA	Bovine serum albumin
Hb	Hemoglobin
PCM	Phase change material
AIPH	2,2′-azobis[2-(2-imidazolin-2-yl)propane]dihydrochloride

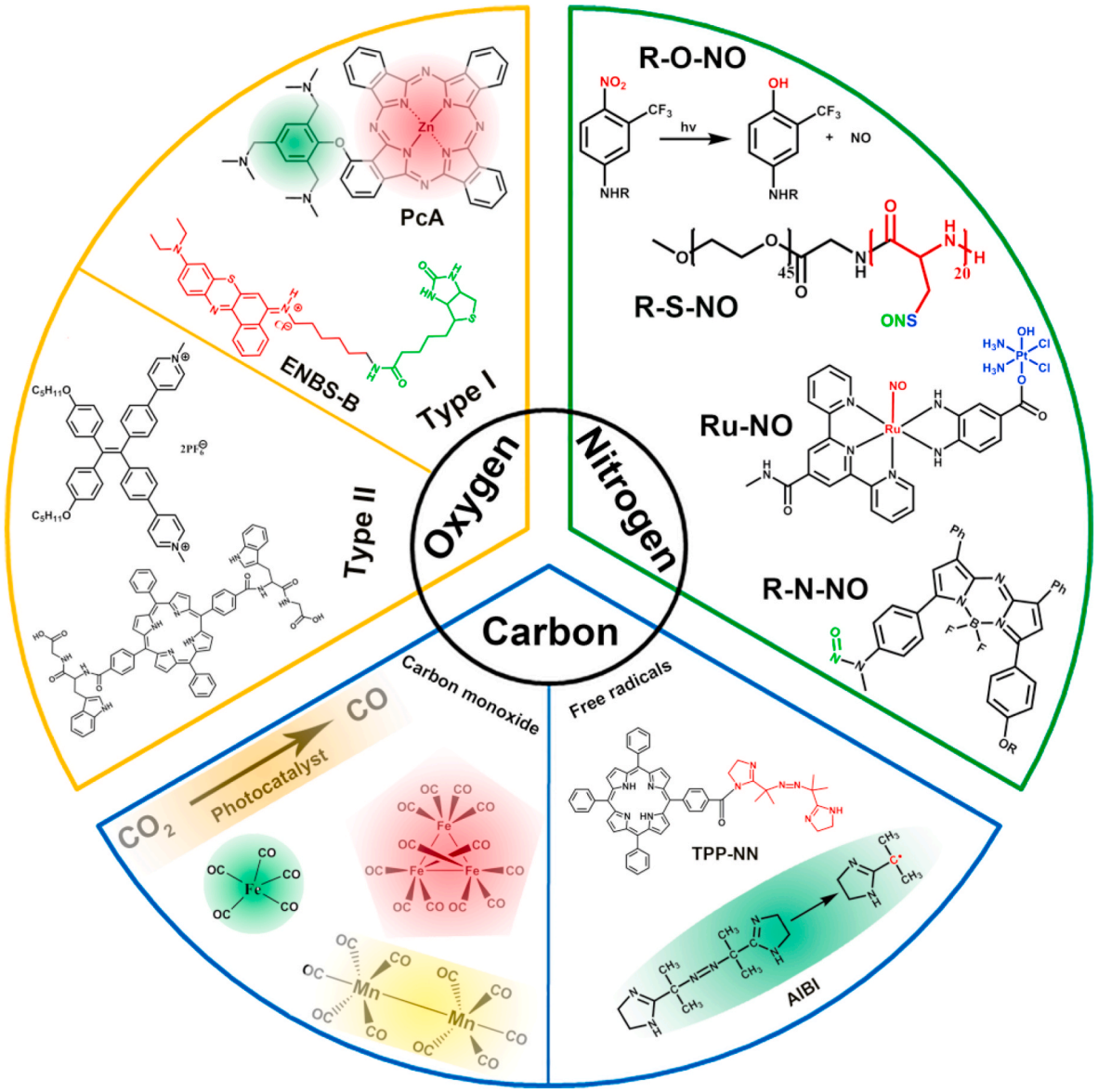

Scheme 1. Schematic illustration of the photoactivatable nanogenerators of reactive species including reactive oxygen, reactive nitrogen, and reactive carbon species for cancer therapy.

reactive species-based monotherapy or the featured synergistic therapy with other therapeutic strategies.

The formation of reactive species in cells can originate from internal and external stimuli. The internal stimuli are specifically derived from some metabolic processes [27–32], or pathological conditions [33]. The external triggers are mainly starting from a range of physicochemical or biochemical reactions induced by reactive species generators. Growing bodies of the experimental data indicated that reactive species generators activated by light irradiation are excellent therapeutic candidates due to their noninvasiveness and spatiotemporally controllable profile in biomedical applications [34]. In this review, we first summarized the recent advances of photo-activatable nanogenerators for reactive species including reactive oxygen species, reactive nitrogen species, and reactive carbon species (Scheme 1). We then discussed the principles for the design of photoactivatable nanoplatforms and their application for cancer therapy. We finally provided our perspectives for improving the therapeutic effect and promoting the clinical translation of the photo-activatable nanoparticles.

2. Reactive oxygen species-based antitumor therapy

Reactive oxygen species (ROS) is composed of reactive radicals or non-radical molecules evolved from oxygen atoms. It is a collective term including singlet oxygen ($^1O_2$), superoxide radical anion ($O_2^{\bullet-}$), hydroxyl radical ($^{\bullet}OH$), hydrogen peroxide (H_2O_2) [35]. ROS can destroy tumor cells through multifactorial mechanisms, including oxidizing the biological macromolecules, destroying angiogenesis to cut off the supply of nutrients to tumor cells [36,37]. Typically, five therapeutic strategies including radiation therapy [38–41], chemodynamic therapy [42–46], sonodynamic therapy [47–50], bioreductive chemotherapeutics (e.g., tirapazamine, TPZ) [51–54], and photodynamic therapy (PDT) [55–62] can generate ROS. Among all these approaches, PDT-based cancer therapies have been extensively exploited.

PDT can be generally classified into oxygen-independent type-I and oxygen-dependent type-II mechanisms. The type-II PDT procedure can transform the photon energy to the photosensitizers (PSs) by exciting the PSs from the ground state to the singlet state. The excited singlet state PSs can further be converted to an excited triplet state through the intersystem crossing process. The excited triplet state PSs eventually transfer the photo energy to the molecular oxygen for generating singlet oxygen ($^1O_2$). In contrast, the type-I PDT can generate superoxide radical anions and hydrogen peroxide without the involvement of molecular oxygen (Fig. 1). The occurrence ratio of the two types of PDT is determined by the types of PSs and the concentration of the environment oxygen [63]. Furthermore, PDT can induce both apoptotic and necrotic death of the tumor cells. Notably, the dying tumor cells crack the plasma membrane and spill out the cytosolic constituents for provoking the inflammatory response, which can activate the protective immune response and suppress tumor growth via recruiting the tumor-infiltrating cytotoxic T lymphocytes [64]. In this section, we mainly discuss the advance of PDT-triggered reactive species generation with the nanogenerators.

2.1. Photoactivatable nanoparticles for Type-II PDT of cancer

Given the successful application of hematoporphyrin for PDT, extensive efforts have been devoted to designing various PSs and exploring their biomedical application. Up to date, both inorganic and organic nanomaterials have been exploited for PDT. The inorganic nanomaterials display superior colloidal stability in the physiological milieu [65–70]. The organic PSs harbor the special merits of good biocompatibility and biodegradability. Various organic nanomaterial-based PSs, such as porphyrin [71–75], boron dipyrromethene (BODIPY) [76–78], cyanine dyes [79–82], aggregation-induced emission (AIE) molecules [83–90], have attracted considerable attention.

The hydrophobic properties lead to the aggregation tendency of most PSs with π-π stacking structures, which heavily restricted the biomedical application of common PSs molecules. Thanks to the molecular assembly strategies and the discovery of various carriers, these insoluble molecules could be prepared as multifunctional nanotherapeutic nanoplatforms. For instance, Yan et al. constructed a novel type of nanophotosensitize via coordination reaction between metal-binding peptides, Zn^{2+} ions, and PS with multiple weak interactions using a multicomponent self-assembly strategy (Fig. 2a) [91]. The obtained self-assembled nano-phototherapeutics exhibited unique advantages including uniform size distribution, high PS loading efficiency, robust colloidal stability in physiological solution, and prolonged blood circulation time in blood. Unsurprisingly, the self-assembled nano--phototherapeutic displayed quenched photoactivity due to aggregation of PS in physiological conditions. In contrast, their photoactivity was restored inside the tumor cells by responding to acidic pH and elevated glutathione (GSH) expression, which endowed the nanoplatform with tumor-specific and highly efficient PDT of cancer. The self-assembly strategy could efficiently solve the solubility problem of PSs molecules with conjugated structures by forming nanoparticles.

To acquire a favorable therapeutic effect, the nanoplatform should facilitate PSs drugs dwell in the tumor sites. Strategies that empower the nanoplatform with high accumulation and long-term retention at the tumor sites is worthy of being investigated. The solid tumor is of an acidic microenvironment due to glycolysis of the tumor cells. To take the advantage of the acidic tumor microenvironment, Pu et al. prepared a

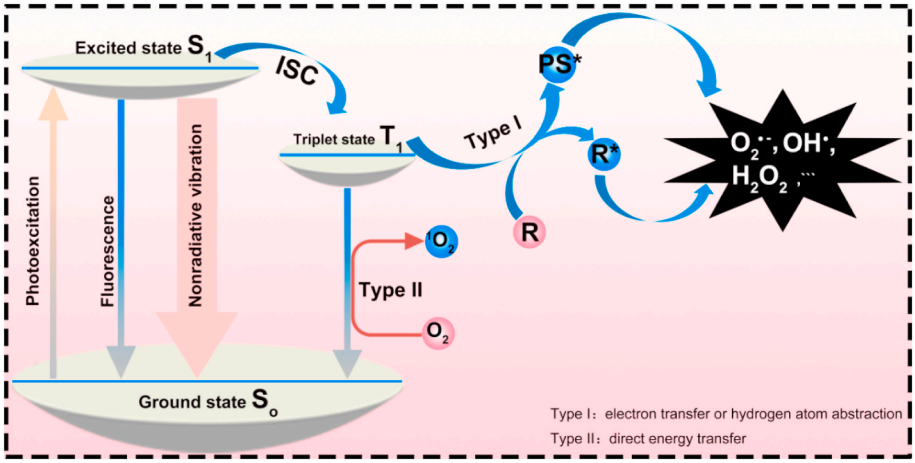

Fig. 1. The mechanisms of type-I and type-II PDT of cancer (R represents the substrate participating in the type-I photochemical reactions, ISC: intersystem crossing).

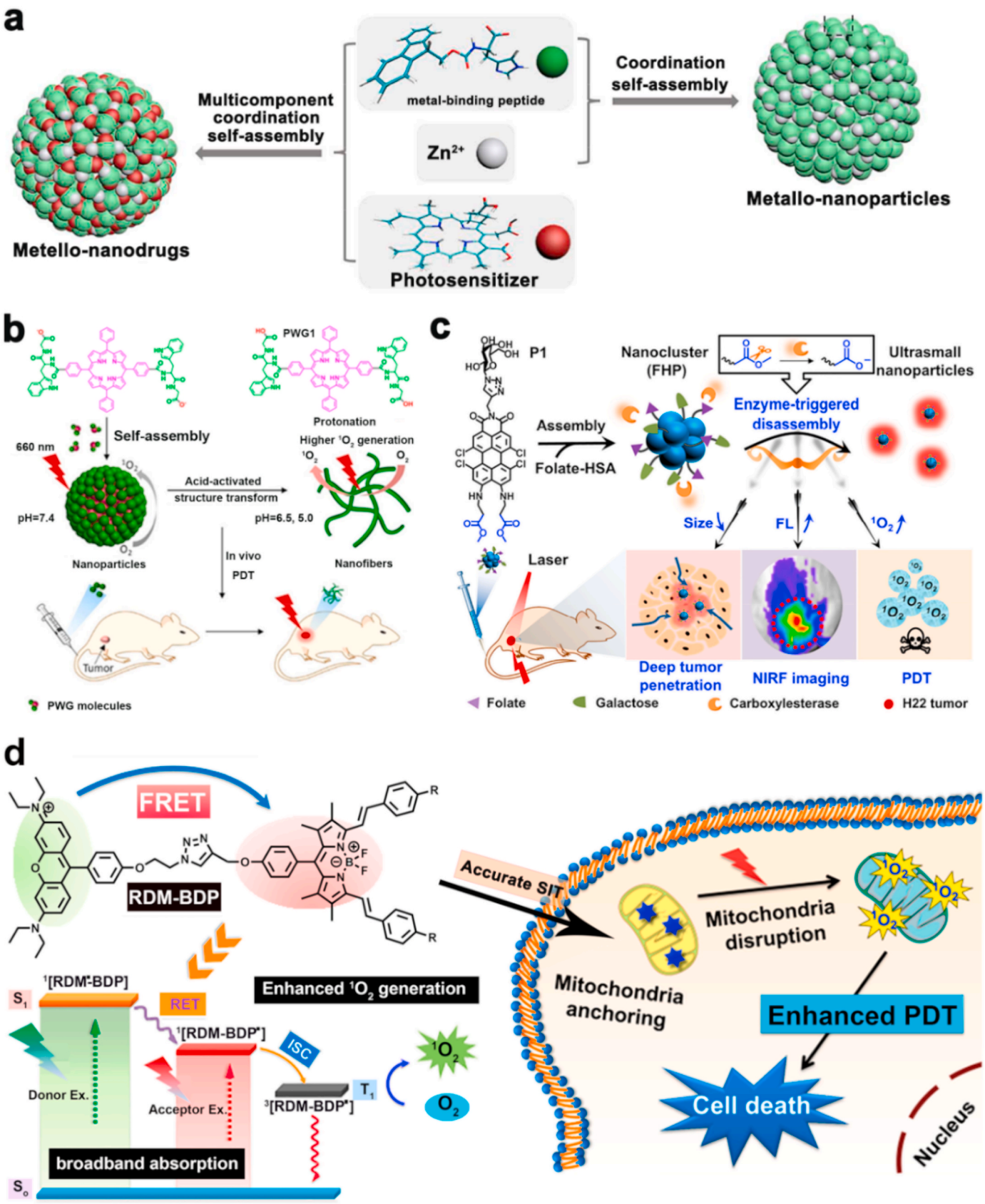

Fig. 2. (a) A schematic diagram of preparing supramolecular metallo-nanodrugs by the coordination of peptide, PSs, and Zn^{2+}. Reprinted with permission [91]. Copyright 2018, American Chemical Society. (b) The transformation of peptide-porphyrin nanoparticles to peptide-porphyrin nanofibers activated by acid and the PDT application after intravenous injection. Reprinted with permission [92]. Copyright 2020, Wiley-VCH. (c) The formation of FHP photoactive nanostructure for NIRF imaging-guided PDT. Reprinted with permission [93]. Copyright 2020, Wiley-VCH. (d) The molecule structure of RDM-BDP for mitochondria targeting PDT. Reprinted with permission [94]. Copyright 2018, American Chemical Society.

kind of self-assembled acid-activated NPs with the peptide-porphyrin conjugates (Fig. 2b) [92]. The obtained peptide-porphyrin conjugate NPs could transform the spheroidal morphology into fibril nanostructure by forming molecular hydrogen bonds under the acidic tumor microenvironment, thereby improving $^1O_2$ generation efficiency and extending tumor accumulation of the nanoparticles. The peptide-porphyrin combined with morphology transformation function displayed excellent PDT performance. In this work, the acid-mediated morphology transformation strategy provided novel ways for elevating the accumulation of nanoparticles in the tumor regions.

To enhance tumor accumulation of the nanomaterials in the deep tissues, the active targeting ligand can be used. Recently, Yin et al. prepared a perylene monoimide-based nanocluster with a size of about 100 nm for fluorescence imaging-guided PDT of deep tumor (Fig. 2c) [93]. In their nanostructure system, the introduction of folate enabled the targeting capability to the tumor sites. The enzyme-triggered hydrolysis reduced the size of the nanostructure, eliciting the formation of ultrasmall NPs with a size of about 10 nm, which promised the successful penetration of NPs into the deep tumor sites. After the hydrolysis-induced disassembly, the fluorescence emission of the nanocluster was recovered, and their $^1O_2$ generation efficiency was also elevated for PDT. Featuring the enzyme-triggered size changes and the modified folate ligand in the structure, the nanoclusters achieved a deep tumor inhibition effect.

To boost the therapeutic index, more strategies elevating the tumor accumulation amount of theranostic materials should be explored. Studies have found that some materials exhibited the nature tumor accumulation tendency due to the presence of delocalized positive charge in their molecular structures. Utilizing the special characteristics, Peng et al. designed a phototheranostic material-based RDM-BDP molecule with the mitochondria-targeting property (Fig. 2d). The smart structure with delocalized positive charges endowed RDM-BDP with the structure-inherent targeting function for enhanced tumor-targeting potency. To further amplify the phototherapeutic outcome, they

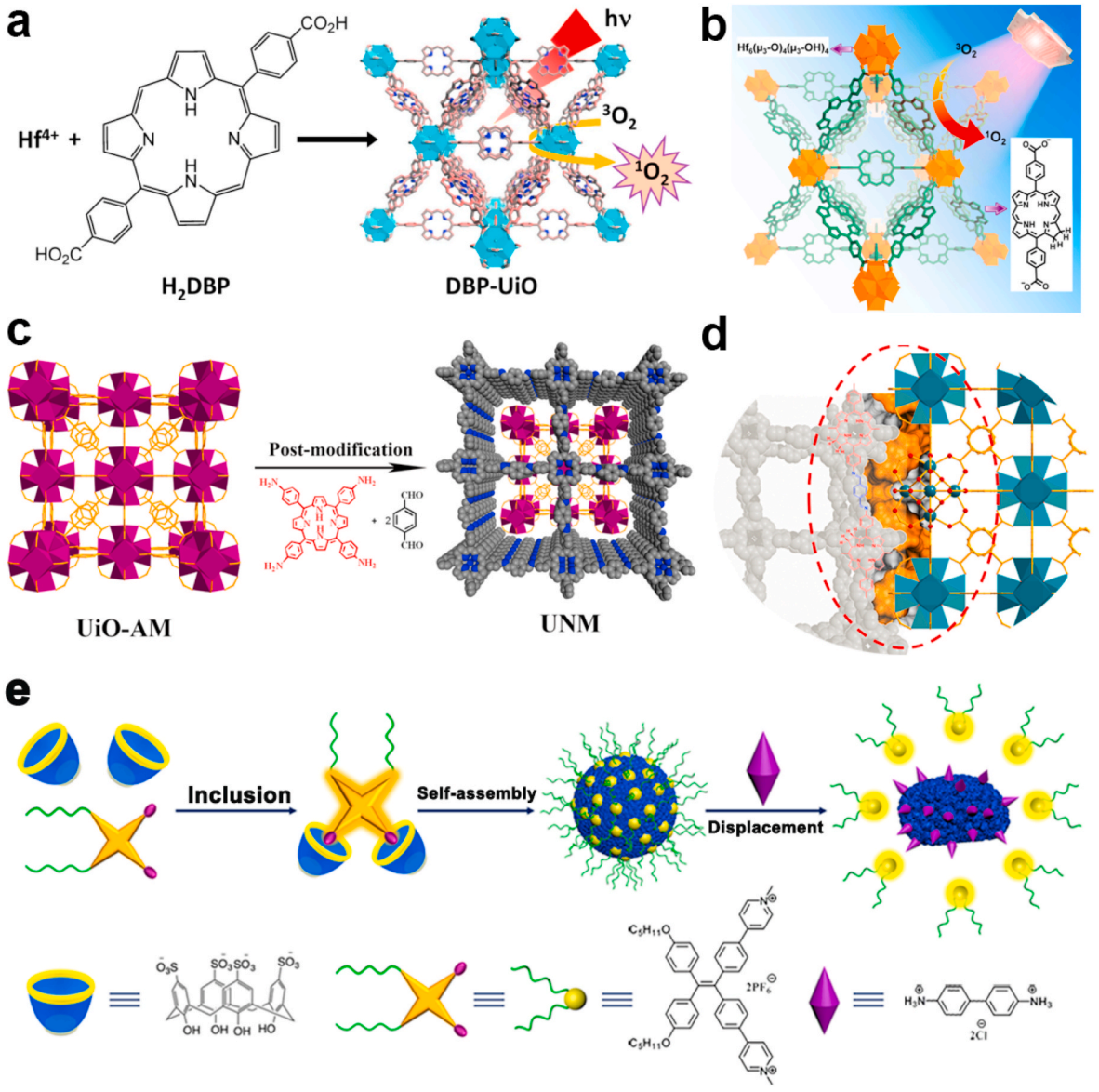

Fig. 3. (a) Synthetic procedure of Hf-DBP NMOF and the $^1O_2$ generation under light illumination. Reprinted with permission [98]. Copyright 2014, American Chemical Society. (b) The structure of DBC-UiO and the photosensitization under light irradiation. Reprinted with permission [99]. Copyright 2015, American Chemical Society. (c) The formation schematic of UNM. Reprinted with permission [102]. Copyright 2017, American Chemical Society. (d) Structure schematic of HUC-PEG. Reprinted with permission [103]. Copyright 2020, Elsevier. (e) A schematic diagram of preparing TPE-PHO nanostructure and the substitution activated phototherapy mechanism. Reprinted with permission [101]. Copyright 2020, American Chemical Society.

introduced the Förster resonance energy transfer (FRET) mechanism into molecular designing. The FRET effect could optimize the photochemical property of PSs by expanding their absorption regions, thus increasing their photon utilization efficiency, and promoting $^1O_2$ generation. Assisted by the structure-inherent targeting function and FRET mechanism, the RDM-BDP-based nanoplatform exhibited notable phototoxicity to cancer cells and remarkable tumor inhibition effect in vivo upon 660 nm laser irradiation [94].

Apart from the above assembly strategies or direct dissolution by the organic solution to solve the hydrophobicity-induced aggregation problem of common PSs, the carriers have been intensively explored. The traditional polymer-carriers cannot completely avoid the aggregation state of hydrophobic molecules, which will partly counteract the photochemical property of photoactive materials. Thanks to the development of materials chemistry, researchers demonstrated that nanoscale metal-organic frameworks (NMOFs) loaded with PSs molecules exhibited great advantage and potential. NMOFs as the vectors of porphyrin derivatives have been extensively employed for cancer therapy [95]. NMOFs with the periodic and ordered structures separate the porphyrin molecules from each other in the framework; thereby avoiding the aggregation caused quenching (ACQ) effect of PSs [96,97]. Moreover, NMOFs are rich in porous structures, which provide passable diffusion channels for the generated reactive species and enhance the antitumor performance of PDT. For instance, Lin et al. fabricated a porphyrin-based NMOF (i.e., DBP-UiO) with plate morphology (Fig. 3a). PDT by DBP-UiO exhibited outstanding antitumor performance toward the drug-resistant tumors under 640 nm light irradiation with a dose of 90 J cm^{-2}. The therapeutic efficacy of DBP-UiO could be attributed to the enhanced $^1O_2$ generation efficiency induced by the heavy atom effect of Hf and ROS diffusion inside the MOF structures [98].

To improve the efficacy of PDT, Lin et al. further built a chlorin-based NMOF (DBC-UiO) with elevated photochemical reactivity and efficiently eliminated the colorectal tumors (Fig. 3b) [99]. The designed DBC-UiO possessed an elevated extinction coefficient in the lowest-energy Q band due to the successful reduction of porphyrin to chlorin [100,101], which endowed the amplified photon-harvesting capability for improved singlet oxygen generation efficiency. The ingenious DBC-UiO with optimized photophysical properties exhibited superior PDT efficacy.

Similar to NMOF, porous organic polymers (POP) integrating porphyrin were also exploited for PDT of cancer. For example, Xie et al. used the core-shell strategy to prepare a nanocomposite (UNM) by combining a metal-organic framework (UiO-66) with a porphyrin-based POP (Fig. 3c) [102]. Upon 450 nm light irradiation with a LED lamp, the porphyrin-based POP produced sufficient $^1O_2$ to kill the tumor cells. Moreover, they demonstrated that chlorin-based POP displayed amplified $^1O_2$ generation ability upon 671 nm laser irradiation (Fig. 3d) [103]. These porous materials-based phototheranostics remarkably inhibited tumor growth.

ACQ phenomenon of the conventional PSs is a major obstacle for hydrophobic nanomaterial-based PDT. In past years, AIE molecules-based nanomaterials have been investigated as alternative phototherapeutic. The AIE molecules can emit fluorescence in an aggregate state and generate cytotoxic $^1O_2$ under laser illumination [87]. Recently, Tang et al. designed a pyridinium-functionalized tetraphenylethylene AIE molecule (TPE-PHO) via host-guest interactions with water-soluble calixarene. The prepared complex structure formed the nanoplatform with supramolecular assembly (Fig. 3e) [101]. In normal conditions, the photoactivity of TPE-PHO was quenched for avoiding dark toxicity during blood circulation. In contrast, the TPE-PHO molecules were competitively replaced by 4,4′-benzidine dihydrochloride from the cavity of calixarene and the photoactivity of TPE-PHO molecules was restored, causing the generation of $^1O_2$ upon white light illumination for PDT at the tumor sites. Moreover, the supramolecular assembly strategy in this work not only facilitates the nanometer form of PSs molecules but also provides the feasible methods for the application of materials with high dark cytotoxicity. Aiming at the hydrophobility problem of photoactive agents, the AIE molecules exhibited great advantage by converting enemies into friends. However, the short absorption wavelength and high dark cytotoxicity presented a formidable challenge to their further in vivo biomedical application.

For oxygen-dependent type II PDT, the inherent tumor hypoxia limitation must be faced and conquered for superior phototherapeutic efficacy. To overcome the hypoxia drawbacks, four pathways have been studied in detail: (1) the direct method is supplying oxygen to the tumor sites utilizing the perfluorocarbon molecules or MnO_2; (2) the employment of hypoxia-activated drugs (such as tirapazamine) can counteract the hypoxia drawback; (3) the way using the decomposition of H_2O_2 for supplying continuous O_2 mediated by some metal-induced catalytic reactions have demonstrated their effectiveness in phototherapy of hypoxic tumors; (4) the introduction of inhibitors towards hypoxia inducing factors can efficiently relieve the hypoxia stress.

To demonstrate this, Chen et al. recently developed an iron-porphyrin MOF-based oxygen-supplying nanoplatform for PDT of cancer. Upon NIR laser irradiation, the nanoparticles were loaded with AuNPs, the latter can catalytic the glucose to generate H_2O_2 via glucose oxidase-like catalytic activity for starvation therapy. Subsequently, the produced H_2O_2 was decomposed to generate oxygen via photocatalysis reaction of Fe-porphyrin constructed MOF (Fig. 4a) [104]. Meanwhile, the porphyrin-based PSs could facilitate the generation of cytotoxic $^1O_2$ excited by the visible light emitted from the UCNPs. This novel system not only provided a continuous source of oxygen for PDT but also used the up-conversion mechanism to convert near-infrared light (980 nm) to visible light, which can solve the tissue-penetration problem of short-wavelength light.

Similarly, Liu et al. used the oxidation etching strategy to prepare holey palladium nanosheets (namely H–Pd NSs) for overcoming the hypoxic tumor microenvironment and improving PDT performance (Fig. 4b) [105]. The palladium nanosheet without etching treatment was employed as a PTT agent. However, the etching decoration endowed the palladium nanosheets with the functionality of catalyzing the decomposition of hydrogen peroxide to generate O_2 (Fig. 4c). The generated O_2 was transferred into $^1O_2$ photocatalyzed by H–Pd NSs upon 808 nm laser irradiation. This oxygen-supplying advantage endowed the nanosystems with similar photoinduced killing efficacy to 4T1 cells under hypoxia and normoxic conditions (Fig. 4d). The combinatory effect of photothermal and PDT, the H–Pd NSs displayed satisfying therapeutic efficacy in vitro and in vivo, which have achieved a tumor inhibition rate of 99.7%.

In addition to the delicate nanoplatform to elevate the oxygen concentration at tumor sites, the direct inhibition of hypoxia-related cascade reactions for enhanced therapeutic effect has been investigated. To relieve the side effects of PDT-induced hypoxic tumor microenvironment, Pu et al. further designed a smart nanoplatform integrating a semi-conducting polymer-based PS and an antagonist of carbonic anhydrase IX (CA-IX) (Fig. 5a) [106]. The CA-IX inhibitor suppressed proliferation and metastasis of the tumor cells by dysregulating the balance of both intracellular and extracellular pH (Fig. 5b). The integration of CA-IX inhibitor enhanced the targeting ability of the whole platform to CA-IX positive breast cancer cells. Upon 680 nm laser irradiation, the semiconducting polymer PS could efficiently produce $^1O_2$ for PDT. By combining the synergistic effect of PDT and anti-tumor metastasis mechanism, a remarkable therapeutic effect could be obtained over monotherapy.

The synergistic therapy could integrate the collective merits of employed multiple treatments and exhibited enhanced therapeutic effect. The introduction of hypoxia-responsive drug systems can efficiently inhibit the tumor cells in hypoxic conditions. For instance, Pu et al. conjugated a chemotherapy drug (IPM-Br) to the backbone of semiconducting polymer nanoparticles (SPNs) via a hypoxia-responsive linker (Fig. 5c) [107]. Upon 808 nm light illumination, the SPNs consumed O_2 to generate $^1O_2$ for PDT. The PDT intensified hypoxia

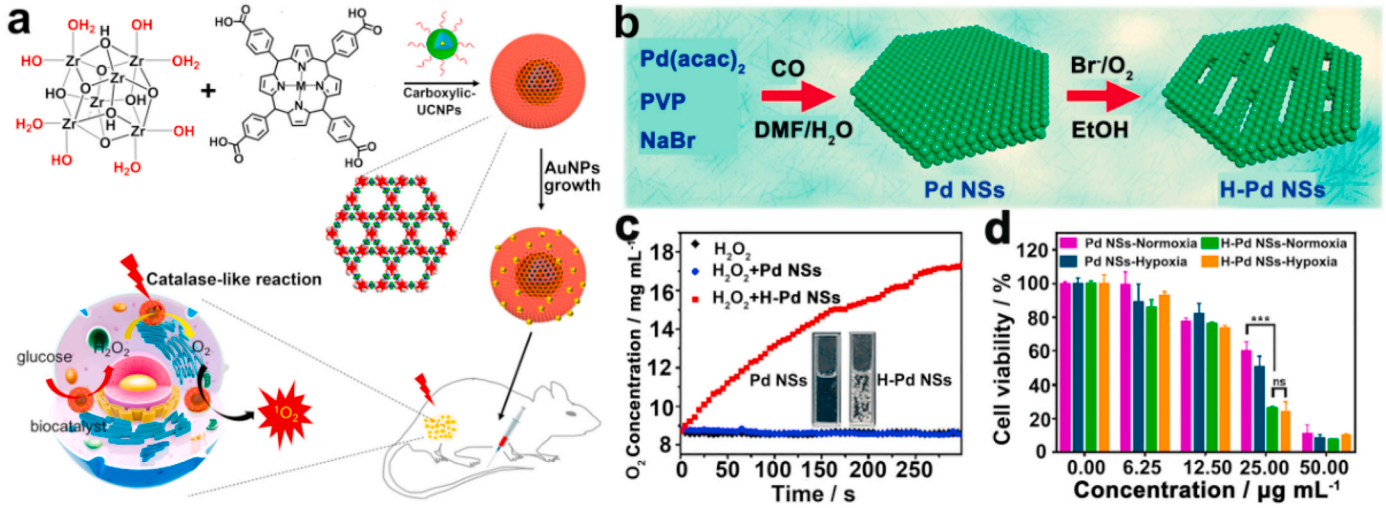

Fig. 4. (a) A schematic diagram of the oxygen self-supplying UMOFs@Au NPs for enhanced PDT efficacy in vivo. Reprinted with permission [104]. Copyright 2020, American Chemical Society. (b) The preparation process of holey Pd NSs (H–Pd NSs). Reprinted with permission [105]. Copyright 2020, American Chemical Society. (c) The detection of the decomposition process of H_2O_2 into O_2 by electron spin resonance spectra. Reprinted with permission [105]. Copyright 2020, American Chemical Society. (d) Viability of 4T1 cells treated with different conditions. Reprinted with permission [105]. Copyright 2020, American Chemical Society.

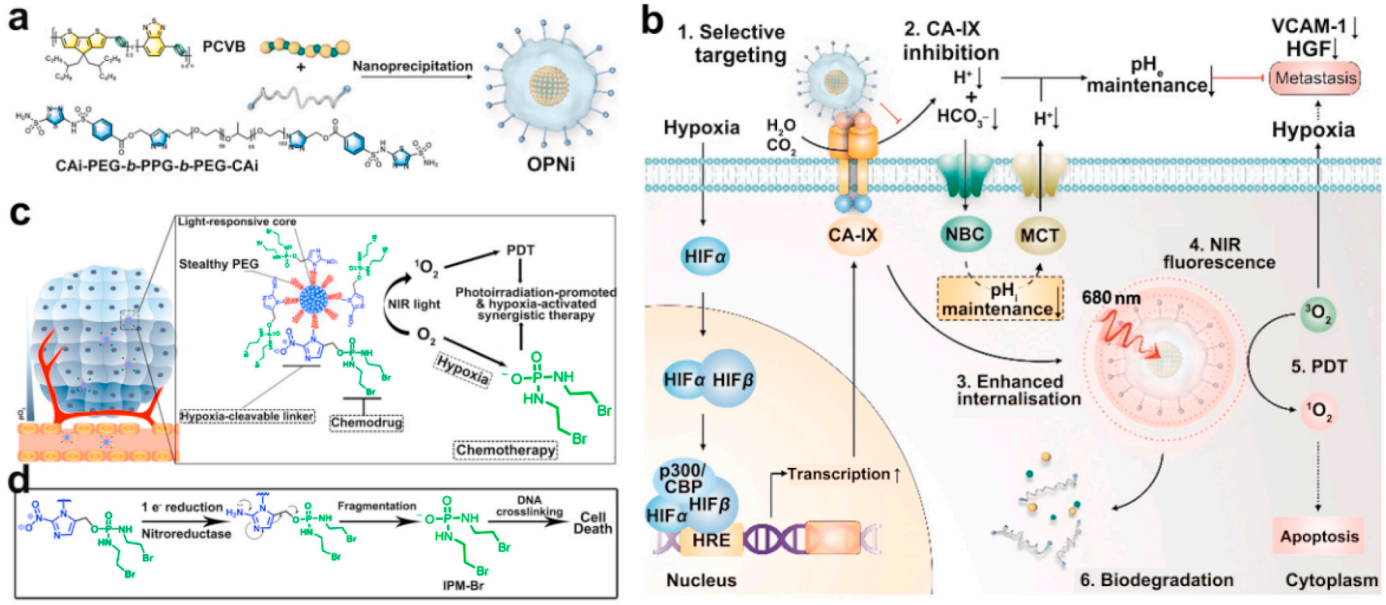

Fig. 5. (a) The preparation of OPNi and (b) the mechanism of OPNi induced synergistic phototherapy. Reprinted with permission [106]. Copyright 2019, Wiley-VCH. (c) The preparation of SPNs photoactive nanomaterials for combined PDT/chemotherapy application. Reprinted with permission [107]. Copyright 2019, Wiley-VCH. (d) The release mechanism of IPM-Br for chemotherapy.

would cleave the hypoxia-sensitive linker and release the IPM-Br drug to crosslink the DNA macromolecules, thereby leading to cellular apoptosis (Fig. 5d). The synergistic PDT and chemotherapy exhibited 4.3-times higher tumor inhibition effectiveness than its chemotherapy process.

2.2. Nanoparticles for Type-I PDT

Just as a Chinese proverb says: "Better to divert rather than blocking and better to change rather than diverting". This motto guides researchers that the hypoxia targeting therapeutic modalities may be better than the direct oxygen-supplying methods, however, the designing of oxygen-independence nanomedicine platforms may possess the optimal therapeutic effect. Thanks to the repaid development of material synthetic chemistry tailed to biomedical application, researchers demonstrated that some photoactivatable nanomaterials could perform type-I PDT in an oxygen-independent manner. These nanomaterials are of great potentials for PDT of hypoxic solid tumors. For example, Huang et al. prepared a novel nanostructure based on the self-assembled phthalocyanine molecules (NanoPcA) (Fig. 6a) [108]. NanoPcA with a unique structure design can avoid the ACQ phenomenon and perform PDT with the type-I mechanism.

Compared with organic nanomaterials-based PSs, metal-based PSs also exhibit remarkable photocytotoxicity in the tumor cells. Recently, Ruiz et al. constructed a PS complex by conjugating the cyclometallated Ir(III) to the coumarin molecules (Ir(III)–COUPY) (Fig. 6b) [109]. Ir(III)–COUPY was effectively endocytosed by HeLa cells and exhibited good biocompatibility in dark conditions. Upon blue or green light irradiation, Ir(III)–COUPY induced a similar photocytotoxicity effect to HeLa cells under normoxic or hypoxic conditions. Mechanism studies indicated that Ir (III)–COUPY caused cell death by generating superoxide

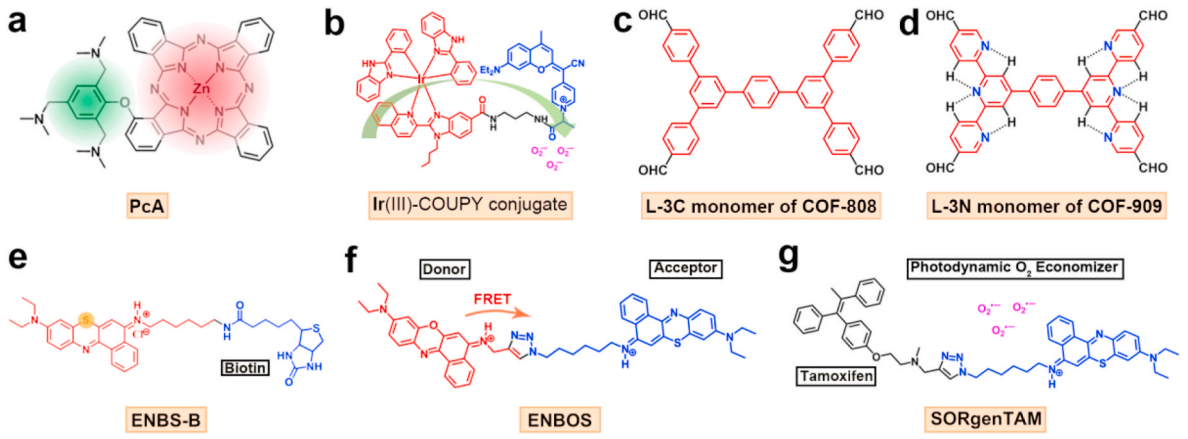

Fig. 6. (a) Molecular structure of PcA. (b) Molecular structure of the Ir(III)–COUPY conjugate. (c) The molecule structure of L-3C for constructing COF-808. (d) The molecule structure of L-3N for constructing COF-909. (e) Molecular structure of ENBS-B. (f) Molecular structure of cationic superoxide radical anion generator-ENBOS. (g) Molecular structure of SORgenTAM.

radical anion after visible light irradiation by performing the type I PDT process under hypoxia conditions. The generated superoxide radical anion could be confirmed by the emitting green fluorescence of dihydrorhodamine 123 (a ROS indicator) in a cell-free-media and the increased luminescence of luminol in the test of a cell-based assay. It is presumed that the Ir(III)–COUPY conjugates selectively produced superoxide radical anion via the possible mechanism of suppressing intramolecular charge recombination. This work excavated the biomedical potential of the cyclometalated Ir(III) complex and coumarin by exploring their cytotoxic $O_2^{\bullet-}$ generation mechanism. The special photochemical behavior could be used to treat hypoxia tumor cells. However, the shorter absorption wavelength of Ir(III)–COUPY conjugates limited their further biomedical application in vivo.

The above PS nanoplatform designing all employed ROS-active motifs as the main photoresponsive group, the ROS-inert motifs could also be favorable photoactivatable agents by forming a special structure. For instance, Deng et al. constructed two kinds of COF nanomaterials (called COF-808 and COF-909) with the photo-inactivatable molecular monomer L-3C (Fig. 6c) and L-3N (Fig. 6d) as building units, respectively [110]. The cross-linked COF-808 and COF-909 generated a large number of superoxide radical anions under 630 nm light irradiation. The generated superoxide radical anions subsequently reacted with the H_2O molecule to form the hydroxyl species. PDT study in vitro showed that COF-909 killed more than 80% of the tumor cells at a concentration as low as 50 μg/mL. The antitumor studies demonstrated that COF-909 inhibited over 90% of tumor growth compared with that of the untreated control group, indicating the promising potential of COF-909 for type-I PDT. However, the clinical translation of these COF structures was restricted by their poor physiological stability.

Besides the traditional nanoparticle mode-based phototherapy, the direct small organic molecules have also been explored as efficient PDT agents. For instance, Peng et al. developed a superoxide radical anion generator (ENBS-B) based on the benzophenothiazine compounds, which could be activated by NIR light (Fig. 6e) [111]. Upon 660 nm laser irradiation, the obtained ENBS-B could produce sufficient $O_2^{\bullet-}$ under light irradiation in a hypoxic environment through the type-I photochemical reaction for PDT (2% O_2). The intracellular uptake amount of ENBS-B was about 87-times higher than the control groups due to the targeting effect of biotin ligands. The generated $O_2^{\bullet-}$ species can destroy the intracellular lysosomes and induced tumor cell apoptosis while participating in SOD-mediated reactions to form H_2O_2 and highly toxic $^{\bullet}OH$. ENBS-B specifically targeted the tumor tissues and efficiently inhibited tumor growth by low-dose laser irradiation when administrated by intravenous injection.

To improve the photochemical property of the nanogenerators, Peng et al. further developed another nanophototherapeutic generating superoxide radical anion ($O_2^{\bullet-}$) for type-I PDT (Fig. 6f) [12]. The photon-absorption capacity of ENBOS in the NIR region was significantly amplified via the FRET mechanism. ENBOS could be activated by laser irradiation at low photodensity. Remarkably, ENBOS displayed excellent "structure inherent targeting" ability. The signal-to-noise ratio of the tumor and surrounding tissues reach 25.2 when administrated by intravenous injection, indicating the excellent tumor targeting ability of ENBOS. Furthermore, ENBOS effectively eliminated the hypoxic tumor owing to the structural intrinsic localization function, strong photon absorption capacity, and oxygen-independence characteristic.

To alleviate the hypoxia burden of tumor cells and acquire more right to use the existing oxygen in the tumor cell, Peng et al. further designed a superoxide radical anion ($O_2^{\bullet-}$) generator (called SORgenTAM), which was able to reverse the hypoxia-induced therapeutic resistance by acting on mitochondrial respiration (Fig. 6g) [112]. Specifically, the tamoxifen molecule in the nanotherapeutic structure affected the normal process of mitochondrial respiration, reduced the hypoxic pressure of tumor cells by preventing O_2 consumption in the tumor cells, and simultaneously down-regulated HIF-1 expression, thereby preventing the tumor cells from becoming hypoxic. The photosensitization studies demonstrated that the superoxide radical anion could transform into hydroxyl radical via a cascade of catalytic reactions. Moreover, the antitumor study suggested that SORgenTAM inhibited self-repair of the tumor cells by activating the AMPK metabolism signaling pathway and enhanced the lethal effect to tumor cells. This study suggested that the SORgenTAM phototherapeutic platform could be tailored for treating deep-seated hypoxia tumors.

2.3. Nanoparticles for combined Type I and II PDT

Thanks to the richness and diversity of existing materials and the advance of synthetic chemistry, researchers have found that some phototherapeutic nanomaterials could simultaneously perform the O_2-dependent and O_2-independent PDT. For instance, Lin et al. developed a Ti-based NMOF (Ti-TBP) for combining Type-I and Type-II PDT process (Fig. 7a) [113]. Upon 650 nm laser irradiation, the Ti-TBP NMOF produced $^1O_2$ and transferred electrons from the excited TBP* species to Ti^{4+}-based secondary building units, generating $TBP^{\bullet+}$ ligands and Ti^{3+} centers, thereby promoting the generation of superoxide anions hydrogen peroxide and hydroxyl radicals. Thus the bifunctional Ti-TBP NMOF nanophototherapeutics-mediated PDT exhibited a superior anticancer effect by generating four different types of ROS and efficiently inhibited the solid tumor growth (~98%) under 650 nm light irradiation.

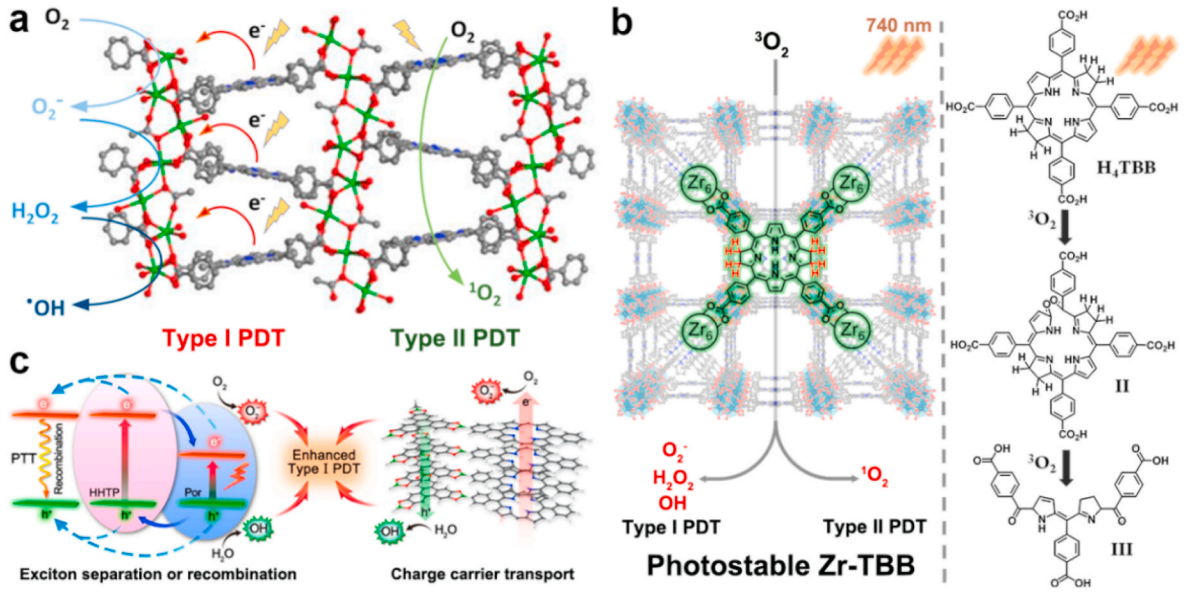

Fig. 7. (a) Schematic structure of Ti-TBP NMOF enabling both types I and type II PDT. Reprinted with permission [113]. Copyright 2019, American Chemical Society. (b) Coordinated complexation of bacteriochlorin ligands and Zr^{4+} to obtain Zr-TBB NMOF for type I and type II PDT. Reprinted with permission [98]. Copyright 2020, American Chemical Society. (c) The mechanism schematic of porphyrin-based 2D CON for PTT and type I PDT. Reprinted with permission [114]. Copyright 2019, American Chemical Society.

To improve the antitumor performance of the nanophototherapeutic, Lin et al. further prepared a Zr-TBB NMOF by utilizing bacteriochlorophyll as the connecting unit and zirconium as the metal node (Fig. 7b) [98]. Under 740 nm laser irradiation, Zr-TBB NMOF triggered superoxide anions, hydrogen peroxide, hydrogen peroxide, and singlet oxygen generation through the type-I and type-II mechanisms, leading to a favorable PDT effect. The four kinds of reactive oxygen species were verified by aminophenyl fluorescein assay and electron paramagnetic resonance measurement. In vivo studies showed that the Zr-TBB NMOF was of excellent antitumor efficacy in the mouse models of breast and colorectal cancer, with cure rates of 40% and 60%, respectively.

In addition to NMOF, covalent organic porous nanostructures gained extensive attention in recent years due to their framework structures and tunable photochemical properties. For instance, Tian et al. prepared a heterogeneous covalent organic nanosheet (CON) with a donor-acceptor structure (Fig. 7c) [114]. Upon 635 nm laser irradiation, the porphyrin PS molecules in the nanosheet generated $^1O_2$ for type-II PDT. Besides, the heterostructure of CONs provided efficient charge separating efficiency to obtain long-lived electrons and holes. Electrons reduced O_2 to form $O_2^{\bullet-}$, and holes oxidized water to produce toxic $^{\bullet}$OH to exert the type-I PDT process. The type-I PDT function significantly relieved the hypoxia-induced resistance to type-II PDT. The CONs displayed significant tumor suppression effect by combining type I, type II PDT and PTT modality when administrated by intravenous injection. This work explored the photochemical mechanism of porphyrin-based CONs and expanded the biomedical application of indissoluble covalent organic nanomaterials.

3. Reactive nitrogen species-mediated tumor suppression

Reactive nitrogen species (RNS) contains nitric oxide ($^{\bullet}$NO) and a wide range of its metabolites, such as peroxynitrite anion ($ONOO^-$) [23,115–118]. As a biological regulatory molecule in the human body, $^{\bullet}$NO plays crucial functions in various physiological and pathological processes [7,8,119]. Therefore, $^{\bullet}$NO is closely related to the occurrence and progression of many diseases including cancer [117]. Similar to reactive oxygen species, $^{\bullet}$NO is a double-edged sword, and its biological effects are concentration-dependent [120]. For instance, $^{\bullet}$NO can promote angiogenesis of the solid tumor at a concentration below 0.2 μmol. In contrast, $^{\bullet}$NO caused poisoning effect in the blood at a concentration of $^{\bullet}$NO higher than 1 μmol [121]. When $^{\bullet}$NO is maintained at a certain concentration (>1 μmol), it could inhibit tumor growth and eventually regressed tumor [122–124]. The main antitumor mechanisms of $^{\bullet}$NO are as follows: (1) affecting the energy metabolism of cancer cells, which resulted in tumor suppression; (2) combining with reactive oxygen radicals (such as superoxide radical anion) in the cell to damage the skeleton structure of DNA by generating nitrogen/oxygen-based free radicals; (3) promoting macrophage activation to fight tumors, and inhibiting tumor metastasis by down-regulating the platelet aggregation; (4) inducing and activating the expression of tumor suppressor gene p53 for causing tumor cell apoptosis; and (5) reducing P-glycoprotein (P-gp) expression levels against drug resistance.

As a typical radical, $^{\bullet}$NO is the source of all RNS in the biological systems [125]. $^{\bullet}$NO possess high reactive activity in the presence of other radicals and exhibit oxidation or nitration potential to the local biomolecules. Therefore, precise cancer therapy can be achieved by controlling $^{\bullet}$NO release at the lesion locations. Generally, there are four bonding strategies including R-O-NO, R-S-NO, R-N-NO (R represents alkyl group), and mental-NO for $^{\bullet}$NO delivery [126]. The four bonding or coordination-based $^{\bullet}$NO supplying nanotherapeutic platforms can achieve light irradiation-triggered $^{\bullet}$NO release. The external light irradiation-induced photothermal effect can also induce a controlled release of $^{\bullet}$NO. However, despite various nanomaterials that have been designed for $^{\bullet}$NO-delivery, it remains a challenge to precisely deliver $^{\bullet}$NO to the tumor sites in a controlled release profile.

$^{\bullet}$NO-based monotherapy application is relatively rare due to the concentration-dependent therapeutic effects of $^{\bullet}$NO. However, NO-based combination therapy has been extensively studied. Current $^{\bullet}$NO-based treatment research mainly focuses on four pathways, including high concentration-induced cytotoxicity [127], as a chemotherapy sensitizer [128], as radiation therapy sensitizer [129], or as phototherapy sensitizer [120,122]. The ever-increasing antitumor research about the combination of $^{\bullet}$NO therapy with various therapeutic strategies demonstrated the great significance of summarizing the related research works. In this section, the mechanism and advantages of synergistic therapy between $^{\bullet}$NO therapy and other therapeutic modalities will be discussed for discovering innovative methods to cure

cancer.

The drug delivery rate for tumor clinical chemotherapy is low due to the limitation of physiological barriers, which lead to poor therapeutic outcomes and tumor metastasis. Studies have shown that a low dose of •NO can amplify the permeability and retention effects (EPR) of the nanoparticles. Moreover, •NO has been extensively employed for sensitizing the tumor cells to chemotherapeutics, such as cisplatin, paclitaxel (PTX), and doxorubicin (DOX). For example, Kim et al. designed a polymer micelle formed by nitrobenzene and platinum prodrugs by conjugating with nitrobenzene molecules at both ends of the platinum prodrugs in the axial direction (Fig. 8a) [128]. The strong hydrophobic property of nitrobenzene improved the loading efficiency of Pt(IV) prodrugs when utilizing polymeric micelles as the carrier. The photo-cleavage of the nitro compound transformed the hydrophobic nitrobenzene into a hydrophilic phenol structure, which further increased the release efficiency of platinum (IV) prodrugs. This nanomedicine platform utilizing •NO donors for tuning •NO release and boosting chemotherapy exhibited effective anticancer effects. However, the tissue penetration of the ultraviolet light is quite limited, which restricted the biomedical application of nitro benzene-based •NO donors in vivo.

Similarly, •NO can be used to amplify the chemosensitivity of PTX by the bonding method of R-S-NO. Li et al. constructed an antitumor nanoplatform (IPH–NO NPs) by utilizing the •NO donor bonded human serum albumin as a drug carrier to support the photosensitizer (IR780) and PTX (Fig. 8b) [130]. IPH-NO NPs slowly released •NO in the presence of glutathione (GSH), thus leading to elevated permeability of NPs to the tumor blood vessels and improved drug accumulation at the tumor sites. Moreover, the NIR light irradiation induced the rapid release of •NO, which directly killed tumor cells, and inhibiting tumor metastasis. This nanoplatform exhibited improved tumor suppression effect and anti-metastasis effect by the synergistic therapy of •NO therapy, photothermal therapy, and chemotherapy.

Also, •NO can be used to enlarge the chemosensitivity of DOX by co-delivery of •NO donor (metal-NO coordination complex) and DOX drugs in one nanoplatform. Shen et al. designed a nanoplatform and proved the positive effect of •NO on DOX-based chemotherapy (Fig. 8c) [131]. In this nanoplatform, chitosan was bonded on the surface of upconversion nanoparticles (UCNPs) and then loading DOX and photoactivated •NO donor (Ruxin black salt, RBS) to obtain the nanospheres (UCNPs (DOX)@CS-RBS) (Fig. 8c). The UCNPs in the nanospheres effectively converted absorbed NIR photons into visible light, triggering the release of •NO. The low pH in the lysosome promoted the release of DOX. They demonstrated that a small dose of •NO acted as a P-gp-mediated therapeutic agent against multidrug resistance (MDR), leading to the increased concentration of DOX in the cell. In the meantime, the high dose of •NO and DOX synergistically killed cancer cells. The combination of DOX and high doses of •NO exhibited an improved tumor proliferation suppression effect. It has been defined that the multidrug resistance had severely limited the therapeutic effect of chemotherapeutic. Therefore, the successful introduction of •NO should be of great practical significance.

In addition to combination with chemotherapy, •NO has also been used to optimize the therapeutic effect of PDT on hypoxia tumors. For instance, Dong and Huang et al. synthesized a nano-PS based on the diketopyrrolopyrrole nucleus (DPP-NF) (Fig. 9a) [122]. They introduced a light-responsive •NO donor (4-nitropyrrole) and pH-sensitive group (dimethylaminophenyl) into the structure of DPP-NF NPs (Fig. 9b). The DPP-NF NPs could be activated under weakly acidic conditions of lysosomes (pH = 4.5–5.0) by forming protonated structure to generate ROS for PDT and enable the photothermal conversion function for PTT under laser irradiation. Moreover, upon 660 nm light illumination, the released •NO was able to trigger tumor cell death by inducing DNA damage. The •NO therapy could overcome the low efficiency of PDT modality to hypoxic tumors. Both in vitro and in vivo antitumor effects demonstrated that DPP-NF NPs are promising phototherapeutic nanoplatform.

It is well known that PDT could suppress tumor growth by causing irreversible oxidative damages to the lipids, amino acids, and proteins. However, some recent evidence have shown that the concentration of •NO synthase (iNOS) was upregulated during the PDT process. The iNOS or •NO donors generated •NO could suppress the PDT-induced

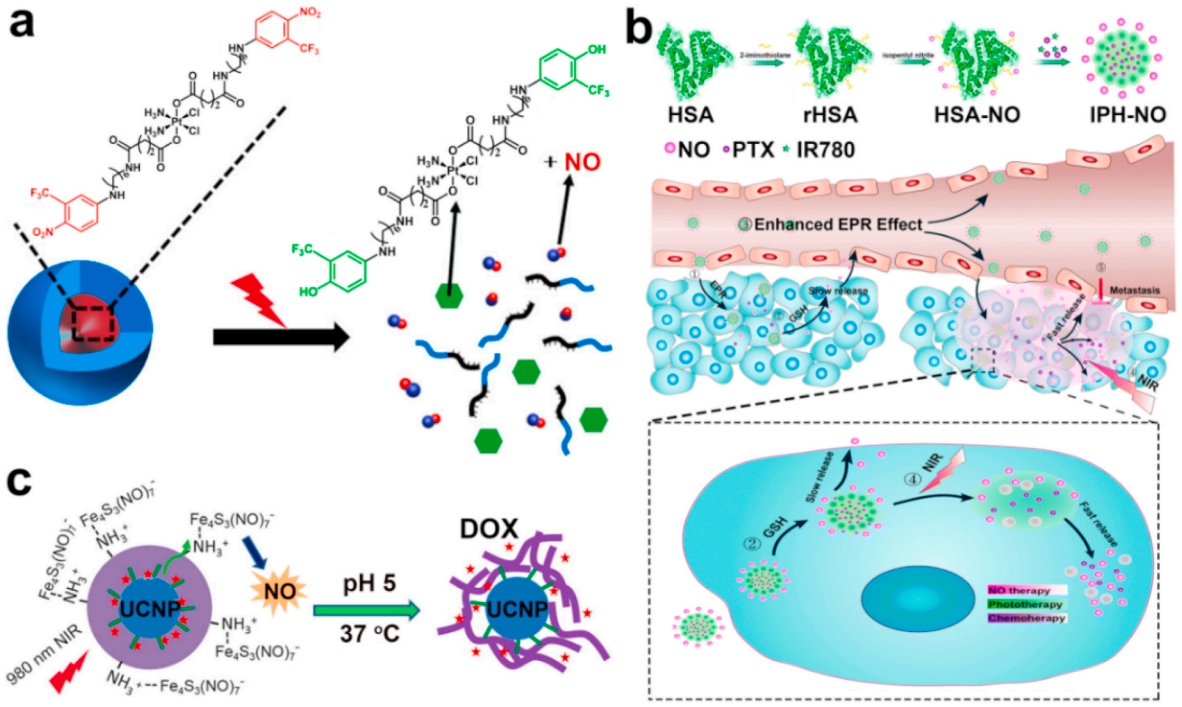

Fig. 8. (a) The structure schematic of the photoactive Pt(IV) prodrug. Reprinted with permission [128]. Copyright 2018, Royal Society of Chemistry. (b) Schematic illustration of the IPH-NO for enhanced antitumor therapy. Reprinted with permission [130]. Copyright 2019, Royal Society of Chemistry. (c) The release mechanism of UCNPs(DOX)@CS-RBS nanomaterials activated by light illumination and the acid. Reprinted with permission [131]. Copyright 2017, Royal Society of Chemistry.

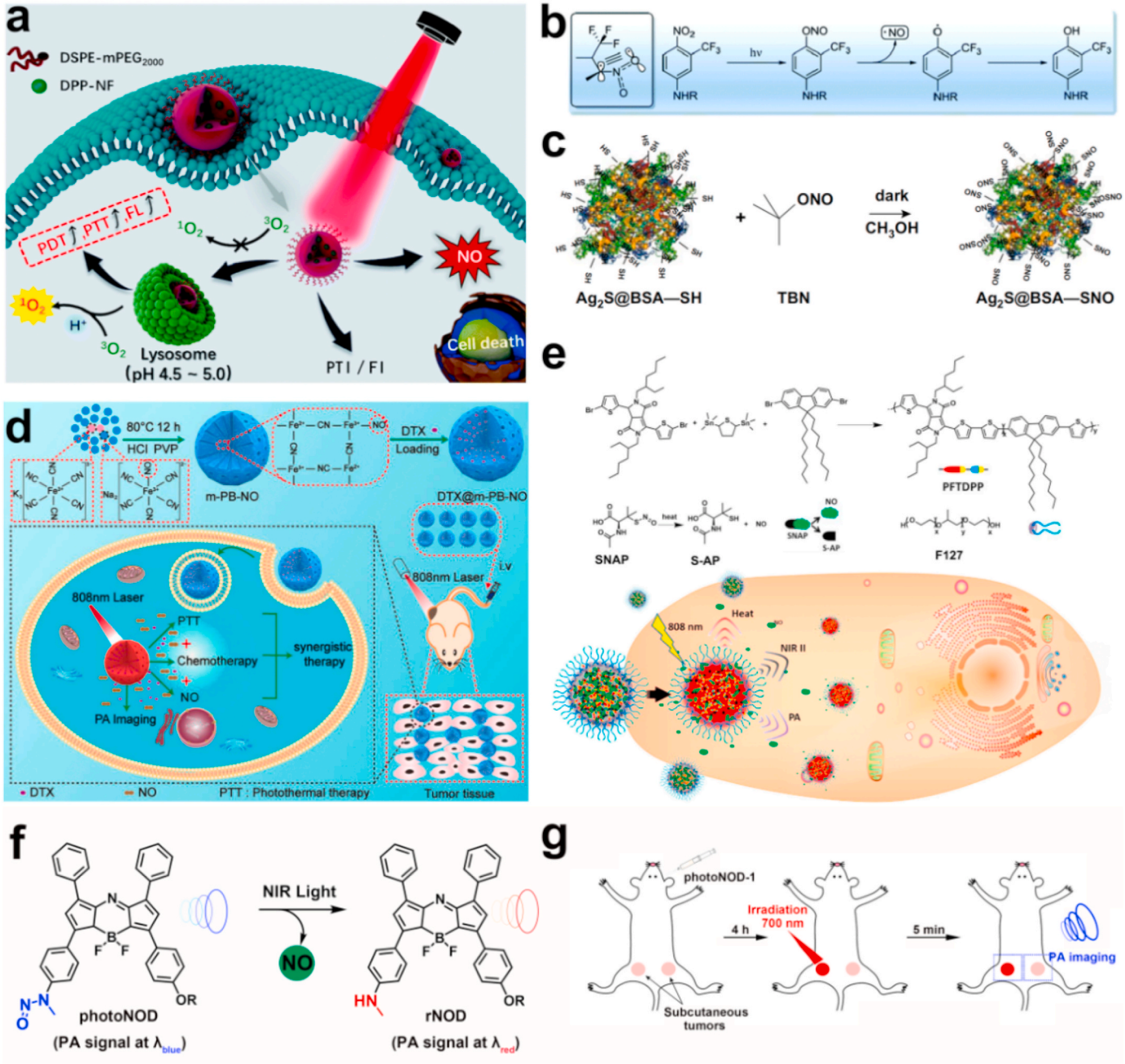

Fig. 9. (a) Schematic illustration of DPP-NF NPs for multifunctional cancer therapy. Reprinted with permission [122]. Copyright 2018, Royal Society of Chemistry. (b) The release mechanism of •NO from DPP-NF NPs. Reprinted with permission [122]. Copyright 2018, Royal Society of Chemistry. (c) The preparation of Ag_2S@BSA-SNO for cancer therapy. Reprinted with permission [129]. Copyright 2020, Springer Nature. (d) The preparation process of m-PB-NO for antitumor therapy. Reprinted with permission [127]. Copyright 2019, Elsevier. (e) PA imaging-guided •NO/photothermal combination therapy. Reprinted with permission [132]. Copyright 2019, Elsevier. (f) Molecule structure of photoNOD and rNOD. (g) PA imaging of photoNOD-1 and release of •NO.

photokilling effect to cancer cells via weakening the lipid peroxidation effect [121]. So the nanomaterials designing about combination of •NO therapy and PDT need to consider more experimental variables to fully understand the function mechanism, thereby obtaining optimal PDT efficacy.

•NO has also been used as an efficient photothermal therapy (PTT) sensitizing agent. Uneven heat distribution often leads to poor accuracy of treatment and side effects of burning normal tissues during the PTT process. Therefore, mild PTT is a considerable alternative and could be explored for antitumor research. Zhao and Gu constructed a nanocomposite based on the bismuth sulfide (Bi_2S_3) NPs and a •NO donor (bis-N-nitroso compound, BNN). Under 808 nm light illumination, BNN released •NO facilitated the even distribution of nanocomposite in solid tumors for mild PTT. Moreover, the exploration result indicated that the self-repair function of tumor cells was inhibited, thus achieving an excellent PTT effect [120]. The results suggested that •NO could cooperate with PTT modality to suppress the growth of tumor cells. This work provided novel insight for avoiding the side effects of hypothermia therapy.

Radiotherapy is commonly used for cancer treatment in the clinic. However, the therapeutic efficiency of radiotherapy is generally unsatisfactory, due to its low specificity, limited drug resistance, and side effects caused by high doses of radiation. Researchers have found that •NO can effectively sensitizer radiotherapy. For instance, Wang et al.

recently synthesized a controlled therapeutic platform by using bovine serum albumin (BSA) as a carrier of Ag_2S quantum dots, $^{\bullet}$NO donors (TBN), and ovalbumin (OVA) (Fig. 9c) [129]. The photothermal effect of the nanoplatform upon 808 nm light irradiation precisely triggered the release of $^{\bullet}$NO, which optimized the radiotherapy effects of heavy metal-Ag and immunotherapy effect induced by OVA. The antitumor study in vivo showed that the survival rate of tumor-bearing mice reached 100% after the treatment of this multifunctional nanoplatform. Compared with the control group, the tumor volume of the $^{\bullet}$NO-combining treatment group was the smallest, indicating the radiotherapy sensitization effect of $^{\bullet}$NO.

In addition to the adjuvant function to other therapy modalities, $^{\bullet}$NO can directly improve tumor treatment efficacy at sufficient concentration. For example, Zhang and Feng have doped $^{\bullet}$NO donor (sodium nitroprusside, SNP) into the mesoporous Prussian blue (m-PB) NPs to obtain m-PB-NO NPs, and then loading docetaxel (DTX) to construct the DTX@m-PB-NO platform (Fig. 9d) [127]. By adjusting the intensity and time of NIR light irradiation (808 nm), $^{\bullet}$NO was released in a controlled manner. This system combined $^{\bullet}$NO therapy, PTT, and chemotherapy to effectively inhibit tumor growth and metastasis. Similarly, Fan et al. used F127 to encapsulate semiconducting polymer and s-nitrosothiol group (SNAP) to form a theranostic platform (Fig. 9e) [132]. Upon 808 nm laser irradiation, the encapsulated semiconducting polymer converted light to heat energy for PTT treatment. The generated heat decomposed s-nitrosothiol to produce $^{\bullet}$NO for cooperative treatment of $^{\bullet}$NO and PTT. The combined treatment strategy inhibited the tumor growth up to a 77% percentage. The synergistic therapy by combining $^{\bullet}$NO and PTT modality has great potential due to the favorable antitumor efficacy.

Along with the therapeutic effect of $^{\bullet}$NO, Chan et al. recently synthesized a $^{\bullet}$NO donor (photoNOD) for photoacoustic (PA) imaging by using aza-BODIPY as the backbone [133]. This NIR light provided enough energy to break the N-nitroso bonds, which helped BODIPY molecules to generate a strong PA signal under excitation, and the photophysical properties were also affected by the change of chemical structure. This NIR light-controlled property enabled the molecule to be an ideal ratiometric probe. After NIR irradiation, photoNOD-1 and photoNOD-2 released $^{\bullet}$NO and generated aza-BODIPY (rNOD-1 or rNOD-2) (Fig. 9f). The conversion from electron-deficient N-nitroso bond to electron-rich N–H bond caused the absorbance redshift of the molecule. The irradiation of photoNOD and rNOD with two wavelengths of light led to the generation of two corresponding PA signals, and the generated ratio signals could detect the ratio of photoNOD and rNOD and non-invasively monitor the release of $^{\bullet}$NO in living animal tissues. Compared with a fluorescence-based imaging modality, PA imaging of photoNOD offered a non-invasive and high-resolution imaging strategy to detect the $^{\bullet}$NO release process without additional contrast agents (Fig. 9g). This work demonstrated that the $^{\bullet}$NO-based reactive species can not only optimize the therapeutic effect of common cancer therapy but also play a part in the imaging field. The potential of $^{\bullet}$NO for PA imaging will be beneficial for performing tunable and tumor-specific $^{\bullet}$NO delivery with the $^{\bullet}$NO donors-containing nanomaterials.

4. Carbon-containing reactive species for cancer therapy

Carbon-containing reactive species are kinds of carbon-centric derivatives. Herein, we mainly overviewed the advances of CO and alkyl radicals-based carbon-containing reactive species for cancer therapy [4].

4.1. CO-performed cancer therapy

It is well known that the binding affinity of CO for hemoglobin (Hb) is 220-times higher than that of oxygen [134,135]. Therefore, CO can disrupt the oxygen-carrying capacity of Hb in the blood, thus causing poisoning effects. CO can also inhibit the function of mitochondria and induce autophagy of the cells. However, CO is a metabolite of endogenous heme. As an endogenous signaling molecule, CO has a variety of biomedical functions, such as regulating blood pressure, reducing inflammation, sensitizing the tumor cells to chemotherapy, and dysfunctionalizing mitochondrial aerobic breathing energy supply [134]. Based on these functionalities, the study of CO as a therapeutic agent has received widespread attention [136,137]. However, to avoid the toxicity of CO, it is essential to deliver CO specifically to the tumor sites and release the payload on demand. Currently, various nanocarriers (such as polymers, ferric oxide, silica nanoparticles, Au nanocages (AuNCs), etc.) have been developed to support the CO donors (Ru carbonyl, Fe carbonyl, and Mn carbonyl). In this section, the potential application and mechanism of CO-based multifunctional nanomaterials for antitumor therapy are summarized.

Based on the special functionality, Zhang et al. used AuNCs to support CO donor-iron pentacarbonyl ($Fe(CO)_5$) under anaerobic conditions, avoiding leakage and oxidation during the blood circulation. The iron pentacarbonyl on the surface of Au nanocages could turn into iron oxide under aerobic conditions (Fig. 10a) [138]. Upon 808 nm laser irradiation, Au converted light to heat energy and promoted the decomposition of iron pentacarbonyl into CO and iron. The generated CO interfered with the respiration of mitochondrial, induced autophagy, and damaged the lysosome in cancer cells. Besides, the produced iron and the iron oxide degraded under the weak acidity of the lysosome and underwent Fenton reaction for producing cytotoxic hydroxyl radicals, which further destructed the autolysosomes, and improved the anticancer performance. This study combined the CO therapy with hydroxyl radicals-induced oxidative damage demonstrated the potential of CO species for antitumor therapy.

Apart from utilizing the influence of CO on the function of mitochondrial for tumor regressing, CO could also be employed to enhance the performance of chemotherapy. To overcome the resistance of chemotherapy, small molecule chemosensitizers are used to make tumor cells more sensitive to chemotherapeutics. Studies indicated that CO could act as a chemotherapy sensitizer and also exert the function of anti-inflammatory. For instance, Zhang et al. designed a multifunctional CO nanogenerator based on partially oxidized tin disulfide nanosheets (POS NSs) to inhibit tumor growth and suppress inflammatory response (Fig. 10b) [139]. POS NSs are modified with targeting ligand-functionalized polymers (PEG-cRGD) for improving their tumor specificity. POS NSs can efficiently load DOX to prepare PPOSD due to the large surface area and volume of NS. The resultant PPOSD could catalyze CO_2 to generate CO upon 561 nm laser irradiation, and sensitize the tumor cells to DOX treatment. Moreover, the POS NS in PPOSD can induce hyperthermia effect upon laser irradiation for photothermal ablation of the tumor. The produced CO could reduce the inflammatory response caused by PTT. This study effectively explored the anti-inflammatory function of CO and uncovered its action mechanism.

Similarly, Shen et al. developed the MCM@PEG–CO–DOX NPs by firstly oxidizing the ferrocene compound to obtain carbonized magnetic NPs (MC), and then modifying the surface of MC with iron-based MOF (MIL-100) and utilizing MIL-100 as a carrier for supporting the CO donor-$Mn(CO)_5Br$ and DOX (Fig. 10c) [140]. Upon 808 nm laser irradiation, MC produced photothermal effects for triggering CO and DOX release. The combination of CO with chemotherapy and PTT elicited an excellent tumor suppression effect. The study demonstrated the potential application of CO for improving chemo- and photothermal therapy of cancer.

CO as the anti-inflammatory agent could precisely avoid the reverse effects (i.e., inflammation) of PTT. To verify the feasibility, Zhang et al. used defective tungsten oxide (WO_3) nanosheets (DW NSs) to support carbon dioxide donor-bicarbonate (BC) and then modified their surface with polyethylene glycol (PEG) to make P@DW/BC nanosheets [141]. Upon 808 nm laser irradiation, the DW in P@DW/BC exerted PTT function and converted carbon dioxide (CO_2) into CO via photocatalysis process. Combining the photothermal and anti-inflammation effects of

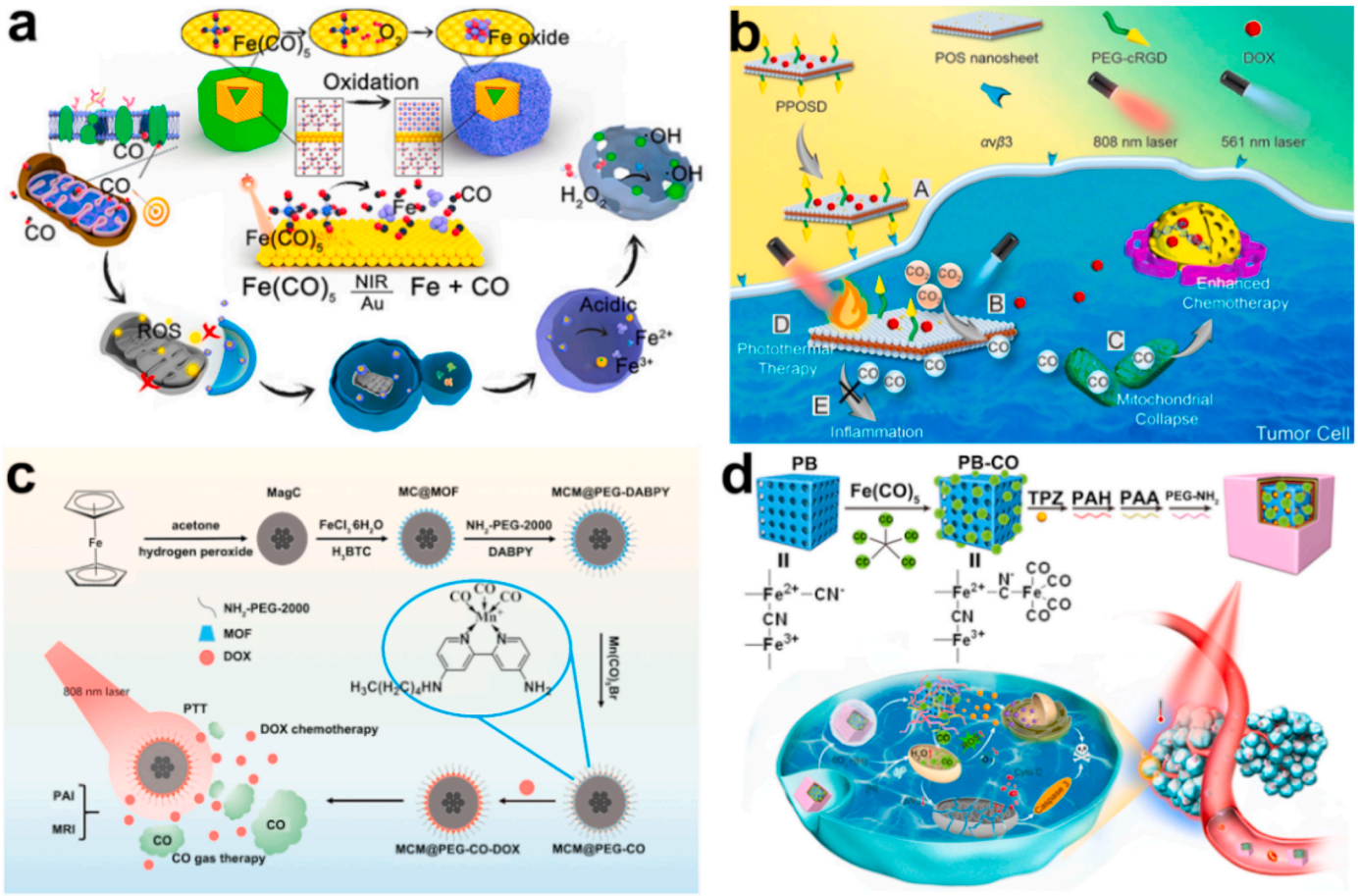

Fig. 10. (a) The antitumor mechanism of $Fe(CO)_5$@Au under laser irradiation. Reprinted with permission [138]. Copyright 2020, American Chemical Society. (b) The photoreduction mechanism of PPOSD and the chemotherapeutic effect of DOX. Reprinted with permission [139]. Copyright 2019, American Chemical Society. (c) The synthetic procedure of MCM@PEG–CO–DOX for antitumor therapy. Reprinted with permission [140]. Copyright 2019, Elsevier. (d) Synthetic schematic of PPPPB-CO-TPZ NPs for antitumor therapy upon laser irradiation. Reprinted with permission [137]. Copyright 2019, Elsevier.

CO, the prepared nanosheets have exhibited excellent antitumor effects with low adverse side effects.

Moreover, recent studies have indicated that CO could accelerate the oxygen consumption of mitochondrial, promoting a hypoxic environment for activating the hypoxia-activatable prodrug. For example, Yin et al. prepared a theranostic nanoplatform by utilizing m-PB NPs as carriers to support the tirapazamine (TPZ) and iron pentacarbonyl ($Fe(CO)_5$, CO donor) (Fig. 10d) [137]. The modification of polyallylamine hydrochloride (PAH) and polyacrylic acid (PAA) on the surface prolonged the blood circulation of the nanoplatform and promoted its accumulation in tumor sites. After intravenous injection, the photothermal effect of PB under 808 nm light irradiation induced the cleavage of the coordination bonds in $Fe(CO)_5$, thus releasing CO. Subsequently, CO accelerated the aerobic respiration of mitochondria and increased the hypoxic extent of tumor cells. The hypoxic environment further activated the bioreductive chemotherapeutic TPZ, which can generate transient oxidative free radicals during the metabolism of reductase to combine with DNA, leading to DNA damage and subsequent cell death. CO-mediated activation of TPZ significantly enhanced the antitumor efficacy of TPZ-mediated chemotherapy. This pioneering study ingeniously explored the influence of CO on the oxygen consumption of mitochondrial and broadened its biomedical application.

Studies have found that the mechanism of multidrug resistance is related to the P-glycoprotein (P-gp)-mediated drug efflux of the cancer cell, and the function of P-gp highly depends on the binding of ATP [142]. There are various strategies to overcome P-gp-involved MDR: (1) using P-gp inhibitors to reduce nicotinamide adenine phosphate dinucleotide (NADPH) and adenosine triphosphate (ATP) to down-regulate P-gp expression. (2) designing anticancer drugs targeting mitochondria and using interfering RNA to silence P-gp expression. Studies have found that CO could reverse the drug resistance of chemotherapy by inactivating mitochondria and suppressing the function of P-gp. For example, Yin et al. reported the strategy of using CO for overcoming the MDR process [143]. They used mesoporous Prussian blue nanoparticles (PB NPs) as a carrier to support iron pentacarbonyl ($Fe(CO)_5$) and DOX. Upon 808 nm laser irradiation, the $Fe(CO)_5$ released CO via photothermal breakdown, resulting in mitochondrial metabolic failure. This process prevented the synthesis of ATP and inhibited ATP-dependent drug outflow, thus reversing drug resistance of MCF-7/ADR tumors. Besides, CO-mediated mitochondrial failure activated the apoptotic protein caspase 3, which further lead to the tumor cell apoptosis.

4.2. *Alkyl radical-mediated cancer inhibition*

ROS can inhibit the proliferation of the tumor cells by inducing oxidative damage to biomolecules (e.g., lipids, proteins, and DNA) and subcellular organelles (i.e., mitochondria). However, the generation of ROS is highly dependent on the local concentration of oxygen. The intratumoral production of ROS is insufficient since most solid tumors are hypoxic, especially the area away from the blood vessels. Therefore, the development of O_2-independent free radical therapy strategies may improve the therapeutic effect by overcoming the hypoxic condition. A feasible method to solve the above problems is delivering free radical-

generating precursors to the tumor sites that can be activated via external stimulation. A recent study showed that 2,2′-azobis[2-(2-imidazolin-2-yl)propane]dihydrochloride (AIPH) as a conventional polymerization initiator can produce alkyl radicals under heat or irradiation activation. The generated free radicals can directly oxidize intracellular components in hypoxia conditions or react with O_2 to produce O_2-containing free radicals, such as alkoxy and peroxy groups in a normoxia microenvironment [144]. AIPH may become an effective biomedical candidate for treating hypoxia tumors.

To achieve tumor-targeted delivery of AIPH, Xia et al. designed a novel nanotherapeutic by integrating AuNC, phase change material (PCM), and AIPH into one single nanoplatform (Fig. 11a) [6]. They used AuNC to load AIPH and wrapped the surface of AuNC with a PCM outer layer. Upon 808 nm laser irradiation, AuNC induced hyperthermia effect for inducing phase transition of PCM and then triggering on-demand AIPH release. As an azo compound, AIPH decomposed rapidly under the stimulation of photothermal-induced heat to generate alkyl radicals. These free radicals directly oxidized cellular components or reacted with oxygen to generate secondary cytotoxic free radicals, including alkoxy and peroxy groups. Even under hypoxic conditions, photothermal-induced heat could still induce AIPH to produce free radicals to increase intracellular lipid hydroperoxide and ultimately lead to oxidation-mediated damage and cell apoptosis. In vitro, experimental results showed that the Au-PCM-AIPH in the hypoxia group and the normoxia group showed an approximate inhibition rate on A549 cells at 61.1% and 62.3%, respectively. The experimental data indicated that the tumor suppression effect of Au-PCM-AIPH was independent of the oxygen level. This novel AIPH-based therapeutic strategy expanded the range of reactive species and extended the biomedicine application of reactive species-based nanomaterials.

Lin et al. further prepared a kind of NPs by combining BSA-coated magnetic Fe_5C_2, AIPH, and PCM (Fig. 11b) [145]. This nanoplatform exhibited a remarkable cancer cell inhibition effect by producing toxic free radicals induced by the photothermal effect. The multifunctional therapeutic nanoplatform also combined magnetic targeting function to remotely control drug delivery. This study combining the alkyl radicles-mediated cancer therapy and the magnetic resonance imaging (MRI) performance could realize the MRI-guided antitumor therapy.

Furthermore, Lin et al. used self-assembly strategies to develop a therapeutic platform based on $CuFeSe_2$ NPs, BSA, and AIPH (Fig. 11c) [146]. Owing to the strong absorption in the NIR-I and NIR-II spectral regions, the $CuFeSe_2$ NPs could activate the release of alkyl radicals and exert a favorable inhibition effect at deep-seated tumor tissues. This work optimized the penetration effect of the photoactivatable nanomaterials and extended the bio-application of reactive species to the deep-seated tumor. Similarly, Qu et al. constructed a theranostic platform by combining AIPH, PCM, and the photoabsorbent PEG-MoS_2 [147]. The designed system could also induce the generation of free radicals under NIR laser irradiation. Results suggested that the MoS_2@AIPH-PCM nanosystem was capable of oxidizing and scavenging GSH inside the tumor cells, thus enhancing the therapeutic effect of alkyl free radicals. This work explored the mechanism of the influence of alkyl radicles on intracellular reducing substances for enhanced antitumor effect.

Organic biomaterials with intrinsic biodegradability have been extensively studied and employed as photothermal inducing agents. For

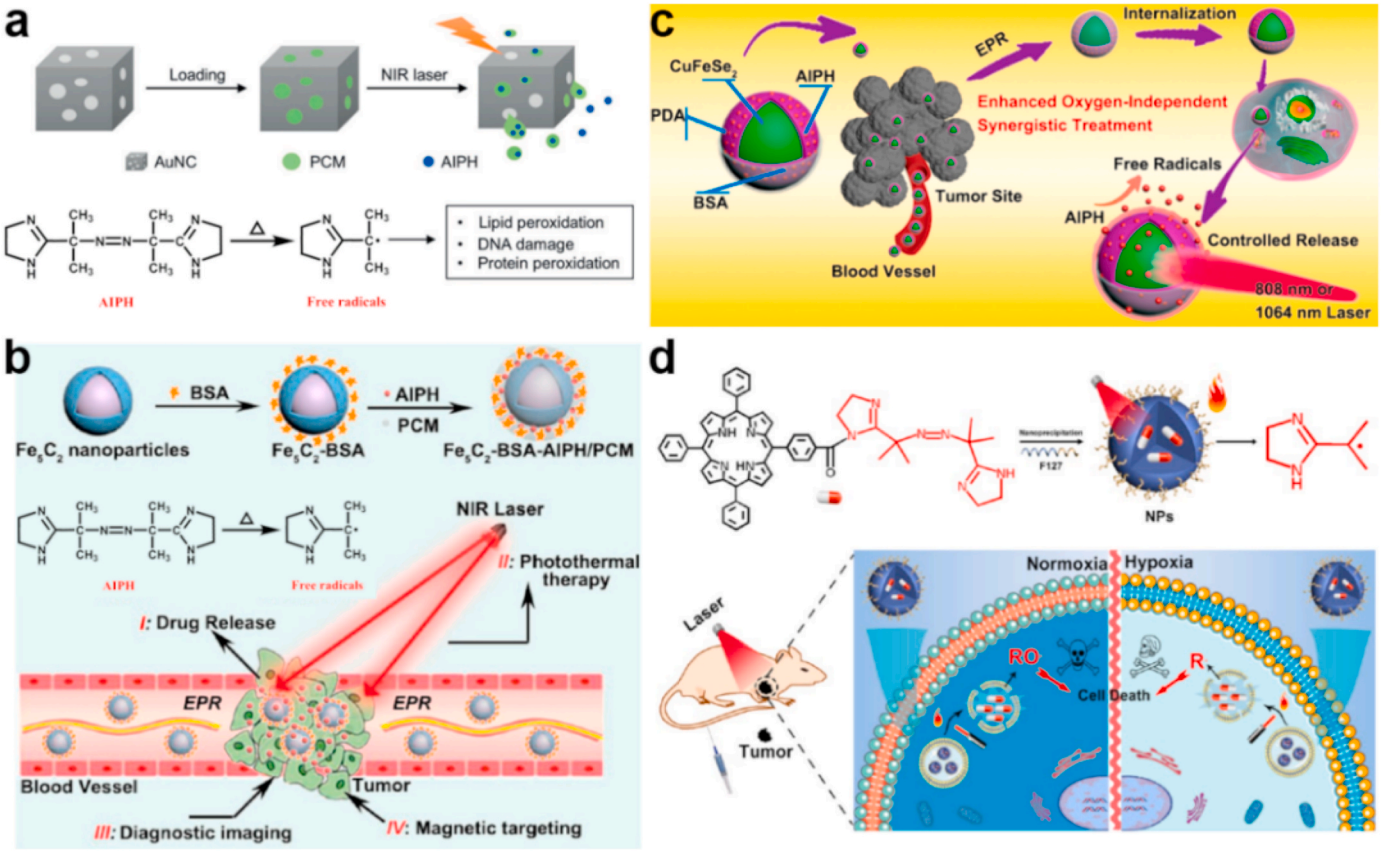

Fig. 11. (a) The reaction mechanism of photo-triggered generation of alkyl radical species. Reproduced with permission [6]. Copyright 2017, Wiley-VCH. (b) The synthetic procedure of Fe_5C_2-BSA-AIPH/PCM for imaging-guided cancer treatment. Reprinted with permission [145]. Copyright 2018, American Chemical Society. (c) Schematic illustration of $CuFeSe_2$-based multifunctional nanomaterials for oxygen-independent synergistic therapy of cancer. Reprinted with permission [146]. Copyright 2019, American Chemical Society. (d) The formulation of TPP-NN NPs and the mechanism of 638 nm laser-triggered generation of alkyl radical species for antitumor therapy. Reprinted with permission [148]. Copyright 2019, American Chemical Society.

example, Xie et al. use Pluronic F-127 to encapsulate a conjugate between porphyrin and AIPH to form the TPP-NN NPs (Fig. 11d) [148]. Under 638 nm laser irradiation, the photothermal effect of porphyrin was transferred to AIPH and induced the generation of alkyl radicals. The generated alkyl radicals could be detected by monitoring the absorbance intensity changes of 1,3-diphenylisobenzofuran in DMF and the enhanced fluorescence from 2′,7′-dichlorodihydrofluorescein in vitro. In vivo tests indicated that TPP-NN NPs could effectively inhibit tumor growth by producing elevated oxidative stress. These results demonstrated the excellent treatment efficacy of alkyl radicals-based reactive species to cancer cells. The work affirmed that the reactive species-based therapeutic strategies have great potential and are necessary to be further vigorously developed.

5. Conclusions and perspectives

In short, this review first discussed the recent development of ROS-based phototherapeutic nanoplatforms for phototherapy and also summarized the advantages or disadvantages of these various nanoplatforms. The photochemical mechanism and materials optimization approaches are introduced in detail for enhanced therapeutic efficacy to tumor cells. Second, the auxiliary functions of •NO to various kinds of therapeutic modalities have been described, which laid the foundation of corresponding synergistic interaction in multifunctional nanomaterials. Third, the in-depth bioapplication mechanism of CO-containing nanoplatforms has been investigated, which holds much promise for the discovery and rational design of precision medicine. Subsequently, the reaction mechanism of photo-triggered generation of alkyl radical species was discussed, which provided innovative direction for biomedical nanomaterials design.

With the rapid development of nanobiotechnology, reactive species-based theranostic has achieved remarkable advances over the past decades [149,150]. Owing to the high controllability and low invasiveness of laser irradiation, photoactivatable nanogenerators have been extensively explored for reactive species-based cancer therapy [123]. Although several reactive species-generating photosensitive drugs have been used clinically, they have not been selected as the first-line treatment due to their intrinsic limitations [35]. The clinically approved reactive species-generators are all oxygen-based photosensitive nanodrugs (5-ALA, Verteporfin, and Porfimer Sodium), and few clinical research data on nitrogen and carbon-based reactive species have been collected. The oxygen-dependence nature of ROS would be doomed to fail to exert ideal therapeutic effects on solid hypoxia tumors. Moreover, the absorption wavelengths of most PSs are below 680 nm. The photo source with a wavelength below 680 nm is difficult to penetrate the deep tumor and activate the PSs distributed inside the tumor tissue [24]. The clinical application of photoactivatable radical species is currently focused on melanoma, lung cancer, and esophageal cancer [96]. For •NO treatment strategies, when nitro is used as a •NO donor, ultraviolet photo source and long-term laser irradiation limit its clinical translation, which required designing more optimized donors to meet the standard of clinical nanomedicine for efficient cancer therapy. For CO treatment, highly tumor-specific delivery of the CO precursor is essential due to strong adhesion between CO and hemoglobin.

Several strategies might be practical to address the above challenges. First, we need to pay more attention to study the therapeutic effects of photoactivatable reactive species, including attempts to treat the in situ tumors and metastatic tumors, as well as injection treatments from mice to larger animals, and systematically evaluating their biological distribution, comprehensive pharmacokinetic pharmacodynamics pathway and other clinical trials, to obtain more useful clinical data. Second, PDT with type I mechanisms should be focused on for treating malignant hypoxic tumors. Oxygen self-supplying drug systems or combining with hypoxia-activated drugs, such as TPZ should be developed. Third, up-conversion materials and two-photon absorption materials could be employed to solve the limitation of light wavelength. Also, the photon absorption capacity can be enhanced by rational molecular chemical designs, and the molecular structure could be smartly designed with high intersystem crossing efficiency from the excited state to the excited triplet state. Furthermore, synergistic therapy methods may endow effective therapeutic effects when the therapeutic outcomes of reactive species based on oxygen, nitrogen, and carbon are ineffective. Notably, due to the huge advantage of immunotherapy in individualized treatment, we must vigorously explore the immunoregulatory potential of reactive species-based nanomedicines [151–154]. Given the safety issues of •NO and CO, it is a prerequisite to constructing nano-pharmaceutical systems with a more precisely controlled release profile. Besides, imaging detection strategies based on different reactive species can help qualitatively and quantitatively monitor the reactive species' biodistribution and corresponding redox state, thus precisely controlling their beneficial treatment and relieving the systemic side effects [155–157].

It is noted that biosafety is a major concern for developing nanotherapeutics. The reactive species-generators comprise a diverse range of photoactivable nanomaterials or nanoparticles. The nanoformulations need to be thoroughly optimized [158]. The sense of biosafety and biocompatibility is crucial for developing radical species-based nanomedicine [159–165]. Multiple discipline collaboration, in particularly the integration of nanotechnology with medicinal chemistry and pharmaceutical technology is important to promote the clinical translation of the photoactivatable nanomedicine for reactive species-based cancer therapy.

Declaration of competing interest

The authors declare no conflict of interest.

Acknowledgments

This work was financially supported by the National Natural Science Foundation of China (31900990 and 51873228), the International Cooperation Project of Science and Technology Commission of Shanghai Municipality (20430711800), and the Scientific Research Foundation of Nantong University (135420623085).

References

[1] S.S. Lucky, K.C. Soo, Y. Zhang, Nanoparticles in photodynamic therapy, Chem. Rev. 115 (2015) 1990–2042.
[2] X. He, Y. Yang, Y. Guo, S. Lu, Y. Du, J.-J. Li, X. Zhang, N.L.C. Leung, Z. Zhao, G. Niu, S. Yang, Z. Weng, R.T.K. Kwok, J.W.Y. Lam, G. Xie, B.Z. Tang, Phage-guided targeting, discriminative imaging, and synergistic killing of bacteria by aie bioconjugates, J. Am. Chem. Soc. 142 (2020) 3959–3969.
[3] L. Wu, A.C. Sedgwick, X. Sun, S.D. Bull, X.-P. He, T.D. James, Reaction-based fluorescent probes for the detection and imaging of reactive oxygen, nitrogen, and sulfur species, Acc. Chem. Res. 52 (2019) 2582–2597.
[4] J. Ohata, K.J. Bruemmer, C.J. Chang, Activity-based sensing methods for monitoring the reactive carbon species carbon monoxide and formaldehyde in living systems, Acc. Chem. Res. 52 (2019) 2841–2848.
[5] R. Weinstain, T. Slanina, D. Kand, P. Klán, Visible-to-nir-light activated release: from small molecules to nanomaterials, Chem. Rev. 120 (2020) 13135–13272.
[6] S. Shen, C. Zhu, D. Huo, M. Yang, J. Xue, Y. Xia, A hybrid nanomaterial for the controlled generation of free radicals and oxidative destruction of hypoxic cancer cells, Angew. Chem. Int. Ed. 56 (2017) 8801–8804.
[7] Y. Deng, F. Jia, S. Chen, Z. Shen, Q. Jin, G. Fu, J. Ji, Nitric oxide as an all-rounder for enhanced photodynamic therapy: hypoxia relief, glutathione depletion and reactive nitrogen species generation, Biomaterials 187 (2018) 55–65.
[8] C.A. Ferreira, D. Ni, Z.T. Rosenkrans, W. Cai, Scavenging of reactive oxygen and nitrogen species with nanomaterials, Nano Res 11 (2018) 4955–4984.
[9] A. Murugan, K.R. Gorantla, B.S. Mallik, D.S. Sharada, Iron promoted c3-h nitration of 2h-indazole: direct access to 3-nitro-2h-indazoles, Org. Biomol. Chem. 16 (2018) 5113–5118.
[10] Z. Guo, Y. Xie, J. Xiao, Z.-J. Zhao, Y. Wang, Z. Xu, Y. Zhang, L. Yin, H. Cao, J. Gong, Single-atom mn–n4 site-catalyzed peroxone reaction for the efficient production of hydroxyl radicals in an acidic solution, J. Am. Chem. Soc. 141 (2019) 12005–12010.
[11] R. Song, H. Wang, M. Zhang, Y. Liu, X. Meng, S. Zhai, C.-c. Wang, T. Gong, Y. Wu, X. Jiang, W. Bu, Near-infrared light-triggered chlorine radical (.Cl) stress for cancer therapy, Angew. Chem. Int. Ed. 59 (2020) 21032–21040.

[12] M. Li, T. Xiong, J. Du, R. Tian, M. Xiao, L. Guo, S. Long, J. Fan, W. Sun, K. Shao, X. Song, J.W. Foley, X. Peng, Superoxide radical photogenerator with amplification effect: surmounting the achilles' heels of photodynamic oncotherapy, J. Am. Chem. Soc. 141 (2019) 2695–2702.
[13] H.D. Grimes, K.K. Perkins, W.F. Boss, Ozone degrades into hydroxyl radical under physiological conditions, Plant Physiol. 72 (1983) 1016.
[14] C.-H. Huang, D. Xu, L. Qin, T.-S. Tang, G.-Q. Shan, L.-N. Xie, P.-L. Li, L. Mao, J. Shao, B.-Z. Zhu, Unexpected activation of n-alkyl hydroxamic acids to produce reactive n-centered free radicals and DNA damage by carcinogenic chlorinated quinones under normal physiological conditions, Free Radical Biol. Med. 146 (2020) 70–78.
[15] L.A. del Río, L.M. Sandalio, J. Palma, P. Bueno, F.J. Corpas, Metabolism of oxygen radicals in peroxisomes and cellular implications, Free Radical Biol. Med. 13 (1992) 557–580.
[16] P. Kuppusamy, M. Chzhan, K. Vij, M. Shteynbuk, D.J. Lefer, E. Giannella, J. L. Zweier, Three-dimensional spectral-spatial epr imaging of free radicals in the heart: a technique for imaging tissue metabolism and oxygenation, Proc. Natl. Acad. Sci. Unit. States Am. 91 (1994) 3388.
[17] J. Emerit, C. Beaumont, F. Trivin, Iron metabolism, free radicals, and oxidative injury, Biomed. Pharmacother. 55 (2001) 333–339.
[18] R.T. Dean, S. Gieseg, M.J. Davies, Reactive species and their accumulation on radical-damaged proteins, Trends Biochem. Sci. 18 (1993) 437–441.
[19] M. Dizdaroglu, Chemical determination of free radical-induced damage to DNA, Free Radical Biol. Med. 10 (1991) 225–242.
[20] E. Birben, U.M. Sahiner, C. Sackesen, S. Erzurum, O. Kalayci, Oxidative stress and antioxidant defense, World Allergy Organ. J. 5 (2012) 9–19.
[21] V. Lobo, A. Patil, A. Phatak, N. Chandra, Free radicals, antioxidants and functional foods: impact on human health, Phcog. Rev. 4 (2010) 118–126.
[22] J.M. MatÉs, C. Pérez-Gómez, I.N. De Castro, Antioxidant enzymes and human diseases, Clin. Biochem. 32 (1999) 595–603.
[23] M. Valko, D. Leibfritz, J. Moncol, M.T.D. Cronin, M. Mazur, J. Telser, Free radicals and antioxidants in normal physiological functions and human disease, Int. J. Biochem. Cell Biol. 39 (2007) 44–84.
[24] Z. Zhou, J. Song, L. Nie, X. Chen, Reactive oxygen species generating systems meeting challenges of photodynamic cancer therapy, Chem. Soc. Rev. 45 (2016) 6597–6626.
[25] D. Trachootham, J. Alexandre, P. Huang, Targeting cancer cells by ros-mediated mechanisms: a radical therapeutic approach? Nat. Rev. Drug Discov. 8 (2009) 579–591.
[26] H. Pelicano, D. Carney, P. Huang, Ros stress in cancer cells and therapeutic implications, Drug Resist. Updates 7 (2004) 97–110.
[27] R.F. Castilho, A.J. Kowaltowski, A. Meinicke, E.J.H. Bechara, A.E. Vercesi, Permeabilization of the inner mitochondrial membrane by ca2+ ions is stimulated by t-butyl hydroperoxide and mediated by reactive oxygen species generated by mitochondria, Free Radical Biol. Med. 18 (1995) 479–486.
[28] K. Bedard, K.-H. Krause, The nox family of ros-generating nadph oxidases: physiology and pathophysiology, Physiol. Rev. 87 (2007) 245–313.
[29] V. Jaquet, L. Scapozza, R.A. Clark, K.-H. Krause, J.D. Lambeth, Small-molecule nox inhibitors: ros-generating nadph oxidases as therapeutic targets, Antioxid. Redox Signal. 11 (2009) 2535–2552.
[30] M.S. Medow, N. Bamji, D. Clarke, A.J. Ocon, J.M. Stewart, Reactive oxygen species (ros) from nadph and xanthine oxidase modulate the cutaneous local heating response in healthy humans, J. Appl. Physiol. 111 (2011) 20–26.
[31] P. Storz, Mitochondrial ros – radical detoxification, mediated by protein kinase d, Trends Cell Biol. 17 (2007) 13–18.
[32] Y.A. Larasati, N. Yoneda-Kato, I. Nakamae, T. Yokoyama, E. Meiyanto, J.-y. Kato, Curcumin targets multiple enzymes involved in the ros metabolic pathway to suppress tumor cell growth, Sci. Rep. 8 (2018) 2039.
[33] T. Hartney, R. Birari, S. Venkataraman, L. Villegas, M. Martinez, S.M. Black, K. R. Stenmark, E. Nozik-Grayck, Xanthine oxidase-derived ros upregulate egr-1 via erk1/2 in pa smooth muscle cells; model to test impact of extracellular ros in chronic hypoxia, PloS One 6 (2011), e27531.
[34] B. Yang, Y. Chen, J. Shi, Reactive oxygen species (ros)-based nanomedicine, Chem. Rev. 119 (2019) 4881–4985.
[35] S. Kwon, H. Ko, D.G. You, K. Kataoka, J.H. Park, Nanomedicines for reactive oxygen species mediated approach: an emerging paradigm for cancer treatment, Acc. Chem. Res. 52 (2019) 1771–1782.
[36] Y. Dai, C. Xu, X. Sun, X. Chen, Nanoparticle design strategies for enhanced anticancer therapy by exploiting the tumour microenvironment, Chem. Soc. Rev. 46 (2017) 3830–3852.
[37] Z.-m. Tang, Y.-y. Liu, D.-l. Ni, J.-j. Zhou, M. Zhang, P.-r. Zhao, B. Lv, H. Wang, D.-y. Jin, W.-b. Bu, Biodegradable nanoprodrugs: "Delivering" ros to cancer cells for molecular dynamic therapy, Adv. Mater. 32 (2020) 1904011.
[38] L. Galluzzi, J.M. Bravo-San Pedro, S. Demaria, S.C. Formenti, G. Kroemer, Activating autophagy to potentiate immunogenic chemotherapy and radiation therapy, Nat. Rev. Clin. Oncol. 14 (2017) 247–258.
[39] Y. Fan, W. Tu, M. Shen, X. Chen, Y. Ning, J. Li, T. Chen, H. Wang, F. Yin, Y. Liu, X. Shi, Targeted tumor hypoxia dual-mode ct/mr imaging and enhanced radiation therapy using dendrimer-based nanosensitizers, Adv. Funct. Mater. 30 (2020) 1909285.
[40] Y. Duo, Y. Huang, W. Liang, R. Yuan, Y. Li, T. Chen, H. Zhang, Ultraeffective cancer therapy with an antimonene-based x-ray radiosensitizer, Adv. Funct. Mater. 30 (2020) 1906010.
[41] S. Shi, R. Vissapragada, J. Abi Jaoude, C. Huang, A. Mittal, E. Liu, J. Zhong, V. Kumar, Evolving role of biomaterials in diagnostic and therapeutic radiation oncology, Bioact. Mater. 5 (2020) 233–240.
[42] Z. Tang, Y. Liu, M. He, W. Bu, Chemodynamic therapy: tumour microenvironment-mediated fenton and fenton-like reactions, Angew. Chem. Int. Ed. 58 (2019) 946–956.
[43] Z. Zhao, W. Wang, C. Li, Y. Zhang, T. Yu, R. Wu, J. Zhao, Z. Liu, J. Liu, H. Yu, Reactive oxygen species–activatable liposomes regulating hypoxic tumor microenvironment for synergistic photo/chemodynamic therapies, Adv. Funct. Mater. 29 (2019) 1905013.
[44] Z. Wang, B. Liu, Q. Sun, S. Dong, Y. Kuang, Y. Dong, F. He, S. Gai, P. Yang, Fusiform-like copper(ii)-based metal–organic framework through relief hypoxia and gsh-depletion co-enhanced starvation and chemodynamic synergetic cancer therapy, ACS Appl. Mater. Interfaces 12 (2020) 17254–17267.
[45] W. Xuan, Y. Xia, T. Li, L. Wang, Y. Liu, W. Tan, Molecular self-assembly of bioorthogonal aptamer-prodrug conjugate micelles for hydrogen peroxide and ph-independent cancer chemodynamic therapy, J. Am. Chem. Soc. 142 (2020) 937–944.
[46] X. Chen, H. Zhang, M. Zhang, P. Zhao, R. Song, T. Gong, Y. Liu, X. He, K. Zhao, W. Bu, Amorphous fe-based nanoagents for self-enhanced chemodynamic therapy by re-establishing tumor acidosis, Adv. Funct. Mater. 30 (2020) 1908365.
[47] I. Rosenthal, J.Z. Sostaric, P. Riesz, Sonodynamic therapy-a review of the synergistic effects of drugs and ultrasound, Ultrason. Sonochem. 11 (2004) 349–363.
[48] A.P. McHale, J.F. Callan, N. Nomikou, C. Fowley, B. Callan, Sonodynamic therapy: concept, mechanism and application to cancer treatment, in: J.-M. Escoffre, A. Bouakaz (Eds.), Therapeutic Ultrasound, Springer International Publishing, Cham, 2016, pp. 429–450.
[49] Y. He, S. Hua Liu, J. Yin, J. Yoon, Sonodynamic and chemodynamic therapy based on organic/organometallic sensitizers, Coord. Chem. Rev. 429 (2020) 213610.
[50] S. Son, J.H. Kim, X. Wang, C. Zhang, S.A. Yoon, J. Shin, A. Sharma, M.H. Lee, L. Cheng, J. Wu, J.S. Kim, Multifunctional sonosensitizers in sonodynamic cancer therapy, Chem. Soc. Rev. 49 (2020) 3244–3261.
[51] S. Yang, Z. Tang, C. Hu, D. Zhang, N. Shen, H. Yu, X. Chen, Selectively potentiating hypoxia levels by combretastatin a4 nanomedicine: toward highly enhanced hypoxia-activated prodrug tirapazamine therapy for metastatic tumors, Adv. Mater. 31 (2019) 1805955.
[52] V.L. Silva, A. Kaassis, A. Dehsorkhi, C.-R. Koffi, M. Severic, M. Abdelhamid, D. Nyimanu, C.J. Morris, W.T. Al-Jamal, Enhanced selectivity, cellular uptake, and in vitro activity of an intrinsically fluorescent copper–tirapazamine nanocomplex for hypoxia targeted therapy in prostate cancer, Biomater. Sci. 8 (2020) 2420–2433.
[53] D. Guo, S. Xu, W. Yasen, C. Zhang, J. Shen, Y. Huang, D. Chen, X. Zhu, Tirapazamine-embedded polyplatinum(iv) complex: a prodrug combo for hypoxia-activated synergistic chemotherapy, Biomater. Sci. 8 (2020) 694–701.
[54] E. Arthur-Baidoo, J. Ameixa, P. Ziegler, F. Ferreira da Silva, M. Ončák, S. Denifl, Reactions in tirapazamine induced by the attachment of low-energy electrons: dissociation versus roaming of oh, Angew. Chem. Int. Ed. 59 (2020) 17177–17181.
[55] J.F. Lovell, T.W.B. Liu, J. Chen, G. Zheng, Activatable photosensitizers for imaging and therapy, Chem. Rev. 110 (2010) 2839–2857.
[56] X. Zhang, J. Tang, C. Li, Y. Lu, L. Cheng, J. Liu, A targeting black phosphorus nanoparticle based immune cells nano-regulator for photodynamic/photothermal and photo-immunotherapy, Bioact. Mater. 6 (2021) 472–489.
[57] C. Wang, P. Zhao, G. Yang, X. Chen, Y. Jiang, X. Jiang, Y. Wu, Y. Liu, W. Zhang, W. Bu, Reconstructing the intracellular ph microenvironment for enhancing photodynamic therapy, Mater. Horiz. 7 (2020) 1180–1185.
[58] R. Bonnett, Photosensitizers of the porphyrin and phthalocyanine series for photodynamic therapy, Chem. Soc. Rev. 24 (1995) 19–33.
[59] A. Raza, S.A. Archer, S.D. Fairbanks, K.L. Smitten, S.W. Botchway, J.A. Thomas, S. MacNeil, J.W. Haycock, A dinuclear ruthenium(ii) complex excited by near-infrared light through two-photon absorption induces phototoxicity deep within hypoxic regions of melanoma cancer spheroids, J. Am. Chem. Soc. 142 (2020) 4639–4647.
[60] E.D. Sternberg, D. Dolphin, C. Brückner, Porphyrin-based photosensitizers for use in photodynamic therapy, Tetrahedron 54 (1998) 4151–4202.
[61] Y. Wang, N. Gong, Y. Li, Q. Lu, X. Wang, J. Li, Atomic-level nanorings (a-nrs) therapeutic agent for photoacoustic imaging and photothermal/photodynamic therapy of cancer, J. Am. Chem. Soc. 142 (2020) 1735–1739.
[62] S. Zhou, X. Hu, R. Xia, S. Liu, Q. Pei, G. Chen, Z. Xie, X. Jing, A paclitaxel prodrug activatable by irradiation in a hypoxic microenvironment, Angew. Chem. Int. Ed. 59 (2020) 23198–23205.
[63] B.M. Luby, C.D. Walsh, G. Zheng, Advanced photosensitizer activation strategies for smarter photodynamic therapy beacons, Angew. Chem. Int. Ed. 58 (2019) 2558–2569.
[64] Z. Zhuang, J. Dai, M. Yu, J. Li, P. Shen, R. Hu, X. Lou, Z. Zhao, B.Z. Tang, Type i photosensitizers based on phosphindole oxide for photodynamic therapy: apoptosis and autophagy induced by endoplasmic reticulum stress, Chem. Sci. 11 (2020) 3405–3417.
[65] F. Li, Z. Liang, D. Ling, Smart organic-inorganic nanogels for activatable theranostics, Curr. Med. Chem. 26 (2019) 1366–1376.
[66] S.M. M, S. Veeranarayanan, T. Maekawa, S.K. D, External stimulus responsive inorganic nanomaterials for cancer theranostics, Adv. Drug Deliv. Rev. 138 (2019) 18–40.
[67] W. Wang, C. Hao, M. Sun, L. Xu, X. Wu, C. Xu, H. Kuang, Peptide mediated chiral inorganic nanomaterials for combating gram-negative bacteria, Adv. Funct. Mater. 28 (2018) 1805112.

[68] Y.-Y. Wang, Y.-C. Liu, H. Sun, D.-S. Guo, Type i photodynamic therapy by organic–inorganic hybrid materials: from strategies to applications, Coord. Chem. Rev. 395 (2019) 46–62.
[69] Z. Xu, X. Chen, Z. Sun, C. Li, B. Jiang, Recent progress on mitochondrial targeted cancer therapy based on inorganic nanomaterials, Mater. Today Chem. 12 (2019) 240–260.
[70] C. Zhang, X. Wang, J. Du, Z. Gu, Y. Zhao, Reactive oxygen species-regulating strategies based on nanomaterials for disease treatment, Adv. Sci. 8 (2020) 2002797.
[71] A. Gao, B. Chen, J. Gao, F. Zhou, M. Saeed, B. Hou, Y. Li, H. Yu, Sheddable prodrug vesicles combating adaptive immune resistance for improved photodynamic immunotherapy of cancer, Nano Lett. 20 (2020) 353–362.
[72] T. Wang, D. Wang, H. Yu, M. Wang, J. Liu, B. Feng, F. Zhou, Q. Yin, Z. Zhang, Y. Huang, Y. Li, Intracellularly acid-switchable multifunctional micelles for combinational photo/chemotherapy of the drug-resistant tumor, ACS Nano 10 (2016) 3496–3508.
[73] F. Zhou, B. Feng, T. Wang, D. Wang, Q. Meng, J. Zeng, Z. Zhang, S. Wang, H. Yu, Y. Li, Programmed multiresponsive vesicles for enhanced tumor penetration and combination therapy of triple-negative breast cancer, Adv. Funct. Mater. 27 (2017) 1606530.
[74] D. Wang, T. Wang, J. Liu, H. Yu, S. Jiao, B. Feng, F. Zhou, Y. Fu, Q. Yin, P. Zhang, Z. Zhang, Z. Zhou, Y. Li, Acid-activatable versatile micelleplexes for pd-l1 blockade-enhanced cancer photodynamic immunotherapy, Nano Lett. 16 (2016) 5503–5513.
[75] F. Zhou, B. Feng, H. Yu, D. Wang, T. Wang, Y. Ma, S. Wang, Y. Li, Tumor microenvironment-activatable prodrug vesicles for nanoenabled cancer chemoimmunotherapy combining immunogenic cell death induction and cd47 blockade, Adv. Mater. 31 (2019) 1805888.
[76] S.H. Lim, C. Thivierge, P. Nowak-Sliwinska, J. Han, H. van den Bergh, G. Wagnières, K. Burgess, H.B. Lee, In vitro and in vivo photocytotoxicity of boron dipyrromethene derivatives for photodynamic therapy, J. Med. Chem. 53 (2010) 2865–2874.
[77] S.G. Awuah, Y. You, Boron dipyrromethene (bodipy)-based photosensitizers for photodynamic therapy, RSC Adv. 2 (2012) 11169–11183.
[78] Q. Guan, D.-D. Fu, Y.-A. Li, X.-M. Kong, Z.-Y. Wei, W.-Y. Li, S.-J. Zhang, Y.-B. Dong, Bodipy-decorated nanoscale covalent organic frameworks for photodynamic therapy, iScience 14 (2019) 180–198.
[79] X. Zhao, Y. Yang, Y. Yu, S. Guo, W. Wang, S. Zhu, A cyanine-derivative photosensitizer with enhanced photostability for mitochondria-targeted photodynamic therapy, Chem. Commun. 55 (2019) 13542–13545.
[80] Q. Zhang, S. Xu, F. Lai, Y. Wang, N. Zhang, M. Nazare, H.-Y. Hu, Rapid synthesis of γ-halide/pseudohalide-substituted cyanine sensors with programmed generation of singlet oxygen, Org. Lett. 21 (2019) 2121–2125.
[81] B. Feng, Z. Niu, B. Hou, L. Zhou, Y. Li, H. Yu, Enhancing triple negative breast cancer immunotherapy by icg-templated self-assembly of paclitaxel nanoparticles, Adv. Funct. Mater. 30 (2020) 1906605.
[82] Y. Li, Y. Zhou, X. Yue, Z. Dai, Cyanine conjugates in cancer theranostics, Bioact. Mater. 6 (2021) 794–809.
[83] N. Alifu, X. Dong, D. Li, X. Sun, A. Zebibula, D. Zhang, G. Zhang, J. Qian, Aggregation-induced emission nanoparticles as photosensitizer for two-photon photodynamic therapy, Mater. Chem. Front. 1 (2017) 1746–1753.
[84] X. He, B. Situ, M. Gao, S. Guan, B. He, X. Ge, S. Li, M. Tao, H. Zou, B.Z. Tang, L. Zheng, Stereotactic photodynamic therapy using a two-photon aie photosensitizer, Small 15 (2019) 1905080.
[85] D.T. Jayaram, S. Ramos-Romero, B.H. Shankar, C. Garrido, N. Rubio, L. Sanchez-Cid, S.B. Gómez, J. Blanco, D. Ramaiah, In vitro and in vivo demonstration of photodynamic activity and cytoplasm imaging through tpe nanoparticles, ACS Chem. Biol. 11 (2016) 104–112.
[86] G. Jin, G. Feng, W. Qin, B.Z. Tang, B. Liu, K. Li, Multifunctional organic nanoparticles with aggregation-induced emission (aie) characteristics for targeted photodynamic therapy and rna interference therapy, Chem. Commun. 52 (2016) 2752–2755.
[87] Q. Li, Y. Li, T. Min, J. Gong, L. Du, D.L. Phillips, J. Liu, J.W.Y. Lam, H.H.Y. Sung, I.D. Williams, R.T.K. Kwok, C.L. Ho, K. Li, J. Wang, B.Z. Tang, Time-dependent photodynamic therapy for multiple targets: a highly efficient aie-active photosensitizer for selective bacterial elimination and cancer cell ablation, Angew. Chem. Int. Ed. 59 (2020) 9470–9477.
[88] Q. Wan, R. Zhang, Z. Zhuang, Y. Li, Y. Huang, Z. Wang, W. Zhang, J. Hou, B. Z. Tang, Molecular engineering to boost aie-active free radical photogenerators and enable high-performance photodynamic therapy under hypoxia, Adv. Funct. Mater. 30 (2020) 2002057.
[89] W. Xiong, L. Wang, X. Chen, H. Tang, D. Cao, G. Zhang, W. Chen, Pyridinium-substituted tetraphenylethylene salt-based photosensitizers by varying counter anions: a highly efficient photodynamic therapy for cancer cell ablation and bacterial inactivation, J. Mater. Chem. B 8 (2020) 5234–5244.
[90] Y. Yuan, C.-J. Zhang, S. Xu, B. Liu, A self-reporting aie probe with a built-in singlet oxygen sensor for targeted photodynamic ablation of cancer cells, Chem. Sci. 7 (2016) 1862–1866.
[91] S. Li, Q. Zou, Y. Li, C. Yuan, R. Xing, X. Yan, Smart peptide-based supramolecular photodynamic metallo-nanodrugs designed by multicomponent coordination self-assembly, J. Am. Chem. Soc. 140 (2018) 10794–10802.
[92] B. Sun, R. Chang, S. Cao, C. Yuan, L. Zhao, H. Yang, J. Li, X. Yan, J.C.M. van Hest, Acid-activatable transmorphic peptide-based nanomaterials for photodynamic therapy, Angew. Chem. Int. Ed. 59 (2020) 20582–20588.
[93] Y. Cai, D. Ni, W. Cheng, C. Ji, Y. Wang, K. Müllen, Z. Su, Y. Liu, C. Chen, M. Yin, Enzyme-triggered disassembly of perylene monoimide-based nanoclusters for activatable and deep photodynamic therapy, Angew. Chem. Int. Ed. 59 (2020) 14014–14018.
[94] M. Li, S. Long, Y. Kang, L. Guo, J. Wang, J. Fan, J. Du, X. Peng, De novo design of phototheranostic sensitizers based on structure-inherent targeting for enhanced cancer ablation, J. Am. Chem. Soc. 140 (2018) 15820–15826.
[95] C. He, D. Liu, W. Lin, Nanomedicine applications of hybrid nanomaterials built from metal-ligand coordination bonds: nanoscale metal-organic frameworks and nanoscale coordination polymers, Chem. Rev. 115 (2015) 11079–11108.
[96] M. Lismont, L. Dreesen, S. Wuttke, Metal-organic framework nanoparticles in photodynamic therapy: current status and perspectives, Adv. Funct. Mater. 27 (2017) 1606314.
[97] J. Lu, L. Yang, W. Zhang, P. Li, X. Gao, W. Zhang, H. Wang, B. Tang, Photodynamic therapy for hypoxic solid tumors via mn-mof as a photosensitizer, Chem. Commun. 55 (2019) 10792–10795.
[98] T. Luo, K. Ni, A. Culbert, G. Lan, Z. Li, X. Jiang, M. Kaufmann, W. Lin, Nanoscale metal-organic frameworks stabilize bacteriochlorins for type i and type ii photodynamic therapy, J. Am. Chem. Soc. 142 (2020) 7334–7339.
[99] G. Lan, Z. Li, S.S. Veroneau, Y.-Y. Zhu, Z. Xu, C. Wang, W. Lin, Photosensitizing metal-organic layers for efficient sunlight-driven carbon dioxide reduction, J. Am. Chem. Soc. 140 (2018) 12369–12373.
[100] Z. Yang, W. Fan, J. Zou, W. Tang, L. Li, L. He, Z. Shen, Z. Wang, O. Jacobson, M. A. Aronova, P. Rong, J. Song, W. Wang, X. Chen, Precision cancer theranostic platform by in situ polymerization in perylene diimide-hybridized hollow mesoporous organosilica nanoparticles, J. Am. Chem. Soc. 141 (2019) 14687–14698.
[101] H.-T. Feng, Y. Li, X. Duan, X. Wang, C. Qi, J.W.Y. Lam, D. Ding, B.Z. Tang, Substitution activated precise phototheranostics through supramolecular assembly of aiegen and calixarene, J. Am. Chem. Soc. 142 (2020) 15966–15974.
[102] L.D. Elliott, S. Kayal, M.W. George, K. Booker-Milburn, Rational design of triplet sensitizers for the transfer of excited state photochemistry from uv to visible, J. Am. Chem. Soc. 142 (2020) 14947–14956.
[103] M. Kang, C. Zhou, S. Wu, B. Yu, Z. Zhang, N. Song, M.M.S. Lee, W. Xu, F.-J. Xu, D. Wang, L. Wang, B.Z. Tang, Evaluation of structure-function relationships of aggregation-induced emission luminogens for simultaneous dual applications of specific discrimination and efficient photodynamic killing of gram-positive bacteria, J. Am. Chem. Soc. 141 (2019) 16781–16789.
[104] L. He, Q. Ni, J. Mu, W. Fan, L. Liu, Z. Wang, L. Li, W. Tang, Y. Liu, Y. Cheng, L. Tang, Z. Yang, Y. Liu, J. Zou, W. Yang, O. Jacobson, F. Zhang, P. Huang, X. Chen, Solvent-assisted self-assembly of a metal-organic framework based biocatalyst for cascade reaction driven photodynamic therapy, J. Am. Chem. Soc. 142 (2020) 6822–6832.
[105] S. Li, K. Gu, H. Wang, B. Xu, H. Li, X. Shi, Z. Huang, H. Liu, Degradable holey palladium nanosheets with highly active 1d nanoholes for synergetic phototherapy of hypoxic tumors, J. Am. Chem. Soc. 142 (2020) 5649–5656.
[106] Y. Jiang, J. Li, Z. Zeng, C. Xie, Y. Lyu, K. Pu, Organic photodynamic nanoinhibitor for synergistic cancer therapy, Angew. Chem. Int. Ed. 58 (2019) 8161–8165.
[107] D. Cui, J. Huang, X. Zhen, J. Li, Y. Jiang, K. Pu, A semiconducting polymer nano-prodrug for hypoxia-activated photodynamic cancer therapy, Angew. Chem. Int. Ed. 58 (2019) 5920–5924.
[108] X. Li, D. Lee, J.-D. Huang, J. Yoon, Phthalocyanine-assembled nanodots as photosensitizers for highly efficient typei photoreactions in photodynamic therapy, Angew. Chem. Int. Ed. 57 (2018) 9885–9890.
[109] V. Novohradsky, A. Rovira, C. Hally, A. Galindo, G. Vigueras, A. Gandioso, M. Svitelova, R. Bresolí-Obach, H. Kostrhunova, L. Markova, J. Kasparkova, S. Nonell, J. Ruiz, V. Brabec, V. Marchán, Towards novel photodynamic anticancer agents generating superoxide anion radicals: a cyclometalated iriii complex conjugated to a far-red emitting coumarin, Angew. Chem. Int. Ed. 58 (2019) 6311–6315.
[110] L. Zhang, S. Wang, Y. Zhou, C. Wang, X.-Z. Zhang, H. Deng, Covalent organic frameworks as favorable constructs for photodynamic therapy, Angew. Chem. Int. Ed. 58 (2019) 14213–14218.
[111] M. Li, J. Xia, R. Tian, J. Wang, J. Fan, J. Du, S. Long, X. Song, J.W. Foley, X. Peng, Near-infrared light-initiated molecular superoxide radical generator: rejuvenating photodynamic therapy against hypoxic tumors, J. Am. Chem. Soc. 140 (2018) 14851–14859.
[112] M. Li, Y. Shao, J.H. Kim, Z. Pu, X. Zhao, H. Huang, T. Xiong, Y. Kang, G. Li, K. Shao, J. Fan, J.W. Foley, J.S. Kim, X. Peng, Unimolecular photodynamic o2-economizer to overcome hypoxia resistance in phototherapeutics, J. Am. Chem. Soc. 142 (2020) 5380–5388.
[113] G. Lan, K. Ni, S.S. Veroneau, X. Feng, G.T. Nash, T. Luo, Z. Xu, W. Lin, Titanium-based nanoscale metal-organic framework for type i photodynamic therapy, J. Am. Chem. Soc. 141 (2019) 4204–4208.
[114] K. Wang, Z. Zhang, L. Lin, J. Chen, K. Hao, H. Tian, X. Chen, Covalent organic nanosheets integrated heterojunction with two strategies to overcome hypoxic-tumor photodynamic therapy, Chem. Mater. 31 (2019) 3313–3323.
[115] H. Wiseman, B. Halliwell, Damage to DNA by reactive oxygen and nitrogen species: role in inflammatory disease and progression to cancer, Biochem. J. 313 (1996) 17–29.
[116] M. Valko, C.J. Rhodes, J. Moncol, M. Izakovic, M. Mazur, Free radicals, metals and antioxidants in oxidative stress-induced cancer, Chem. Biol. Interact. 160 (2006) 1–40.
[117] I. Liguori, G. Russo, F. Curcio, G. Bulli, L. Aran, D. Della-Morte, G. Gargiulo, G. Testa, F. Cacciatore, D. Bonaduce, P. Abete, Oxidative stress, aging, and diseases, Clin. Interv. Aging 13 (2018) 757–772.

[118] J.M. Fukuto, L.J. Ignarro, In vivo aspects of nitric oxide (no) chemistry: Does peroxynitrite (-oono) play a major role in cytotoxicity? Acc. Chem. Res. 30 (1997) 149–152.
[119] T. Yang, Z. Du, H. Qiu, P. Gao, X. Zhao, H. Wang, Q. Tu, K. Xiong, N. Huang, Z. Yang, From surface to bulk modification: plasma polymerization of amine-bearing coating by synergic strategy of biomolecule grafting and nitric oxide loading, Bioact. Mater. 5 (2020) 17–25.
[120] X. Zhang, J. Du, Z. Guo, J. Yu, Q. Gao, W. Yin, S. Zhu, Z. Gu, Y. Zhao, Efficient near infrared light triggered nitric oxide release nanocomposites for sensitizing mild photothermal therapy, Adv. Sci. 6 (2019) 1801122.
[121] A.W. Girotti, Nitric oxide-mediated resistance to antitumor photodynamic therapy, Photochem. Photobiol. 96 (2020) 500–505.
[122] Y. Wang, X. Huang, Y. Tang, J. Zou, P. Wang, Y. Zhang, W. Si, W. Huang, X. Dong, A light-induced nitric oxide controllable release nano-platform based on diketopyrrolopyrrole derivatives for ph-responsive photodynamic/photothermal synergistic cancer therapy, Chem. Sci. 9 (2018) 8103–8109.
[123] C. Fowley, A.P. McHale, B. McCaughan, A. Fraix, S. Sortino, J.F. Callan, Carbon quantum dot–no photoreleaser nanohybrids for two-photon phototherapy of hypoxic tumors, Chem. Commun. 51 (2015) 81–84.
[124] J.V. Garcia, J. Yang, D. Shen, C. Yao, X. Li, R. Wang, G.D. Stucky, D. Zhao, P. C. Ford, F. Zhang, Nir-triggered release of caged nitric oxide using upconverting nanostructured materials, Small 8 (2012) 3800–3805.
[125] Y. Cao, M. Liu, J. Cheng, J. Yin, C. Huang, H. Cui, X. Zhang, G. Zhao, Acidity-triggered tumor-targeted nanosystem for synergistic therapy via a cascade of ros generation and no release, ACS Appl. Mater. Interfaces 12 (2020) 28975–28984.
[126] P.G. Wang, M. Xian, X. Tang, X. Wu, Z. Wen, T. Cai, A.J. Janczuk, Nitric oxide donors: Chemical activities and biological applications, Chem. Rev. 102 (2002) 1091–1134.
[127] T. Feng, J. Wan, P. Li, H. Ran, H. Chen, Z. Wang, L. Zhang, A novel nir-controlled no release of sodium nitroprusside-doped prussian blue nanoparticle for synergistic tumor treatment, Biomaterials 214 (2019) 119213.
[128] S. Pramanick, J. Kim, J. Kim, G. Saravanakumar, D. Park, W.J. Kim, Synthesis and characterization of nitric oxide-releasing platinum(iv) prodrug and polymeric micelle triggered by light, Bioconjugate Chem. 29 (2018) 885–897.
[129] X. Zhou, Z. Meng, J. She, Y. Zhang, X. Yi, H. Zhou, J. Zhong, Z. Dong, X. Han, M. Chen, Q. Fan, K. Yang, C. Wang, Near-infrared light-responsive nitric oxide delivery platform for enhanced radioimmunotherapy, Nano-Micro Lett. 12 (2020) 100.
[130] Y. Xu, H. Ren, J. Liu, Y. Wang, Z. Meng, Z. He, W. Miao, G. Chen, X. Li, A switchable no-releasing nanomedicine for enhanced cancer therapy and inhibition of metastasis, Nanoscale 11 (2019) 5474–5488.
[131] L. Tan, R. Huang, X. Li, S. Liu, Y.-M. Shen, Controllable release of nitric oxide and doxorubicin from engineered nanospheres for synergistic tumor therapy, Acta Biomater. 57 (2017) 498–510.
[132] J. Li, R. Jiang, Q. Wang, X. Li, X. Hu, Y. Yuan, X. Lu, W. Wang, W. Huang, Q. Fan, Semiconducting polymer nanotheranostics for nir-ii/photoacoustic imaging-guided photothermal initiated nitric oxide/photothermal therapy, Biomaterials 217 (2019) 119304.
[133] E.Y. Zhou, H.J. Knox, C.J. Reinhardt, G. Partipilo, M.J. Nilges, J. Chan, Near-infrared photoactivatable nitric oxide donors with integrated photoacoustic monitoring, J. Am. Chem. Soc. 140 (2018) 11686–11697.
[134] H. Yan, J. Du, S. Zhu, G. Nie, H. Zhang, Z. Gu, Y. Zhao, Emerging delivery strategies of carbon monoxide for therapeutic applications: from co gas to co releasing nanomaterials, Small 15 (2019) 1904382.
[135] L. Chen, S.-F. Zhou, L. Su, J. Song, Gas-mediated cancer bioimaging and therapy, ACS Nano 13 (2019) 10887–10917.
[136] C. Liu, Z. Du, M. Ma, Y. Sun, J. Ren, X. Qu, Carbon monoxide controllable targeted gas therapy for synergistic anti-inflammation, iScience 23 (2020) 101483.
[137] Y. Li, J. Dang, Q. Liang, L. Yin, Carbon monoxide (co)-strengthened cooperative bioreductive anti-tumor therapy via mitochondrial exhaustion and hypoxia induction, Biomaterials 209 (2019) 138–151.
[138] X.-S. Wang, J.-Y. Zeng, M.-J. Li, Q.-R. Li, F. Gao, X.-Z. Zhang, Highly stable iron carbonyl complex delivery nanosystem for improving cancer therapy, ACS Nano 14 (2020) 9848–9860.
[139] S.-B. Wang, C. Zhang, Z.-X. Chen, J.-J. Ye, S.-Y. Peng, L. Rong, C.-J. Liu, X.-Z. Zhang, A versatile carbon monoxide nanogenerator for enhanced tumor therapy and anti-inflammation, ACS Nano 13 (2019) 5523–5532.
[140] J. Yao, Y. Liu, J. Wang, Q. Jiang, D. She, H. Guo, N. Sun, Z. Pang, C. Deng, W. Yang, S. Shen, On-demand co release for amplification of chemotherapy by mof functionalized magnetic carbon nanoparticles with nir irradiation, Biomaterials 195 (2019) 51–62.
[141] S.-B. Wang, C. Zhang, J.-J. Ye, M.-Z. Zou, C.-J. Liu, X.-Z. Zhang, Near-infrared light responsive nanoreactor for simultaneous tumor photothermal therapy and carbon monoxide-mediated anti-inflammation, ACS Cent. Sci. 6 (2020) 555–565.
[142] A. Persidis, Cancer multidrug resistance, Nat. Biotechnol. 17 (1999) 94–95.
[143] Y. Li, J. Dang, Q. Liang, L. Yin, Thermal-responsive carbon monoxide (co) delivery expedites metabolic exhaustion of cancer cells toward reversal of chemotherapy resistance, ACS Cent. Sci. 5 (2019) 1044–1058.
[144] M.C. Krishna, M.W. Dewhirst, H.S. Friedman, J.A. Cook, W. Degraff, A. Samuni, A. Russo, J.B. Mitchell, Hyperthermic sensitization by the radical initiator 2,2′-azobis (2-amidinopropane) dihydrochloride (aaph). I. In vitro studies, Int. J. Hyperther. 10 (1994) 271–281.
[145] L. Feng, S. Gai, Y. Dai, F. He, C. Sun, P. Yang, R. Lv, N. Niu, G. An, J. Lin, Controllable generation of free radicals from multifunctional heat-responsive nanoplatform for targeted cancer therapy, Chem. Mater. 30 (2018) 526–539.
[146] J. Yang, R. Xie, L. Feng, B. Liu, R. Lv, C. Li, S. Gai, F. He, P. Yang, J. Lin, Hyperthermia and controllable free radical coenhanced synergistic therapy in hypoxia enabled by near-infrared-ii light irradiation, ACS Nano 13 (2019) 13144–13160.
[147] S. Wu, X. Liu, J. Ren, X. Qu, Glutathione depletion in a benign manner by mos2-based nanoflowers for enhanced hypoxia-irrelevant free-radical-based cancer therapy, Small 15 (2019) 1904870.
[148] R. Xia, X. Zheng, X. Hu, S. Liu, Z. Xie, Photothermal-controlled generation of alkyl radical from organic nanoparticles for tumor treatment, ACS Appl. Mater. Interfaces 11 (2019) 5782–5790.
[149] M.-X. Wu, Y.-W. Yang, Metal-organic framework (mof)-based drug/cargo delivery and cancer therapy, Adv. Mater. 29 (2017) 1606134.
[150] W. Cai, J. Wang, C. Chu, W. Chen, C. Wu, G. Liu, Metal-organic framework-based stimuli-responsive systems for drug delivery, Adv. Sci. 6 (2019) 1801526.
[151] B. Feng, B. Hou, Z. Xu, M. Saeed, H. Yu, Y. Li, Self-amplified drug delivery with light-inducible nanocargoes to enhance cancer immunotherapy, Adv. Mater. 31 (2019) 1902960.
[152] P. Cheng, Q. Miao, J. Li, J. Huang, C. Xie, K. Pu, Unimolecular chemo-fluoro-luminescent reporter for crosstalk-free duplex imaging of hepatotoxicity, J. Am. Chem. Soc. 141 (2019) 10581–10584.
[153] J. Li, Y. Luo, K. Pu, Electromagnetic nanomedicines for combinational cancer immunotherapy, Angew. Chem. Int. Ed. (2020), https://doi.org/10.1002/anie.202008386.
[154] Z. Zeng, C. Zhang, J. Li, D. Cui, Y. Jiang, K. Pu, Activatable polymer nanoenzymes for photodynamic immunometabolic cancer therapy, Adv. Mater. 33 (2021) 2007247.
[155] P. Cheng, J. Zhang, J. Huang, Q. Miao, C. Xu, K. Pu, Near-infrared fluorescence probes to detect reactive oxygen species for keloid diagnosis, Chem. Sci. 9 (2018) 6340–6347.
[156] J. Huang, J. Huang, P. Cheng, Y. Jiang, K. Pu, Near-infrared chemiluminescent reporters for in vivo imaging of reactive oxygen and nitrogen species in kidneys, Adv. Funct. Mater. 30 (2020) 2003628.
[157] J. Huang, J. Li, Y. Lyu, Q. Miao, K. Pu, Molecular optical imaging probes for early diagnosis of drug-induced acute kidney injury, Nat. Mater. 18 (2019) 1133–1143.
[158] R.H.J. Mathijssen, A. Sparreboom, J. Verweij, Determining the optimal dose in the development of anticancer agents, Nat. Rev. Clin. Oncol. 11 (2014) 272–281.
[159] L. Wang, L. Yan, J. Liu, C. Chen, Y. Zhao, Quantification of nanomaterial/nanomedicine trafficking in vivo, Anal. Chem. 90 (2017) 589–614.
[160] C. Chen, Y.-F. Li, Y. Qu, Z. Chai, Y. Zhao, Advanced nuclear analytical and related techniques for the growing challenges in nanotoxicology, Chem. Soc. Rev. 42 (2013) 8266–8303.
[161] A.C. Anselmo, S. Mitragotri, Nanoparticles in the clinic, Bioeng. Transl. Med. 1 (2016) 10–29.
[162] D. Bobo, K.J. Robinson, J. Islam, K.J. Thurecht, S.R. Corrie, Nanoparticle-based medicines: a review of fda-approved materials and clinical trials to date, Pharm. Res. (N. Y.) 33 (2016) 2373–2387.
[163] H. Chen, W. Zhang, G. Zhu, J. Xie, X. Chen, Rethinking cancer nanotheranostics, Nat. Rev. Mater. 2 (2017) 17024.
[164] H. Chen, Z. Gu, H. An, C. Chen, J. Chen, R. Cui, S. Chen, W. Chen, X. Chen, X. Chen, Z. Chen, B. Ding, Q. Dong, Q. Fan, T. Fu, D. Hou, Q. Jiang, H. Ke, X. Jiang, G. Liu, S. Li, T. Li, Z. Liu, G. Nie, M. Ovais, D. Pang, N. Qiu, Y. Shen, H. Tian, C. Wang, H. Wang, Z. Wang, H. Xu, J.-F. Xu, X. Yang, S. Zhu, X. Zheng, X. Zhang, Y. Zhao, W. Tan, X. Zhang, Y. Zhao, Precise nanomedicine for intelligent therapy of cancer, Sci. China Chem. 61 (2018) 1503–1552.
[165] J.I. Hare, T. Lammers, M.B. Ashford, S. Puri, G. Storm, S.T. Barry, Challenges and strategies in anti-cancer nanomedicine development: an industry perspective, Adv. Drug Deliv. Rev. 108 (2017) 25–38.